

LA-5931

23

c.1

UC-33

Reporting Date: March 1975

Issued: June 1975

# A Review of Fuel Element Development for Nuclear Rocket Engines

by

J. M. Taub

**For Reference**

**Not to be taken from this room**



**Los Alamos**  
**scientific laboratory**  
of the University of California  
LOS ALAMOS, NEW MEXICO 87544

An Affirmative Action/Equal Opportunity Employer

UNITED STATES  
ENERGY RESEARCH AND DEVELOPMENT ADMINISTRATION  
CONTRACT W-7405-ENG. 36

Work partially supported by the National Aeronautics  
and Space Administration.

Printed in the United States of America. Available from  
National Technical Information Service  
U.S. Department of Commerce  
5285 Port Royal Road  
Springfield, VA 22151  
Price: Printed Copy \$5.45 Microfiche \$2.25

This report was prepared as an account of work sponsored  
by the United States Government. Neither the United States  
nor the United States Energy Research and Development Ad-  
ministration, nor any of their employees, nor any of their con-  
tractors, subcontractors, or their employees, makes any  
warranty, express or implied, or assumes any legal liability or  
responsibility for the accuracy, completeness, or usefulness of  
any information, apparatus, product, or process disclosed, or  
represents that its use would not infringe privately owned  
rights.



3 9338 00374 2615

## CONTENTS

I.	INTRODUCTION .....	1
II.	REACTOR DESIGN .....	3
III.	KIWI-A .....	5
IV.	MATERIALS AND FABRICATION PROCEDURES .....	5
	A. KIWI-A Prime .....	5
	B. Types of Fuel Particles .....	7
	C. Typical Processing Equipment .....	7
	D. Raw Materials .....	8
	1. Graphite Flour .....	8
	2. Carbon Black .....	10
	3. Flake Graphite .....	10
	4. Uranium Dioxide .....	10
	5. Coated UC <sub>2</sub> Particles .....	11
	6. Thermosetting Resin .....	11
	7. Catalyst .....	11
	E. Blending and Extrusion .....	12
	F. Heat Treatments .....	15
	1. KIWI-A through -B4D Oxide-Loaded Elements .....	15
	2. KIWI-B4E, Phoebus 1 and 2, and Pewee-1 Coated-Particle Loaded Elements .....	16
V.	MACHINING AND INSPECTION .....	17
VI.	FUEL ELEMENT COATING .....	18
	A. KIWI-A and -A Prime .....	18
	B. KIWI-B Series .....	20
	C. Phoebus and Pewee Series .....	21
	D. Nuclear Furnace-1 .....	23
VII.	NONDESTRUCTIVE TESTING .....	23
VIII.	NUCLEAR SAFETY .....	25
IX.	FUEL ELEMENT AND TIP JOINING .....	26
	A. Gluing .....	26
	B. Brazing .....	26
X.	FUEL ELEMENT EVALUATION .....	27
	A. Hot-Gas Testing .....	27
	B. Thermal Stress Testing .....	29
XI.	ADVANCED FUEL ELEMENTS .....	30
	A. High-CTE Graphite Elements .....	30
	B. Composite Elements .....	31
	C. Carbide Elements .....	37

XII. FUEL ELEMENT PROPERTIES .....	37
A. Unfueled Graphite .....	39
B. Fueled Graphite .....	39
C. Composite Fuels .....	39
XIII. SUMMARY .....	41
REFERENCES .....	42
APPENDIX. ROVER AND NERVA TESTS AT NRDS .....	45

# A REVIEW OF FUEL ELEMENT DEVELOPMENT FOR NUCLEAR ROCKET ENGINES

by

J. M. Taub

## ABSTRACT

The Los Alamos Scientific Laboratory (LASL) entered the nuclear propulsion field in 1955 and began work on all aspects of a nuclear propulsion program involving uranium-loaded graphite fuels, hydrogen propellant, and a target exhaust temperature of  $\sim 2500^{\circ}\text{C}$ . A very extensive uranium-loaded graphite fuel element technology evolved from the program. Selection and composition of raw materials for the extrusion mix had to be coupled with heat treatment studies to give optimum element properties. The highly enriched uranium in the element was incorporated as  $\text{UO}_2$ , pyrocarbon-coated  $\text{UC}_2$ , or solid solution  $\text{UC}\cdot\text{ZrC}$  particles. An extensive development program resulted in successful NbC or ZrC coatings on elements to withstand hydrogen corrosion at elevated temperatures. Hot gas, thermal shock, thermal stress, and NDT evaluation procedures were developed to monitor progress in preparation of elements with optimum properties. Final evaluation was made in reactor tests at NRDS. Aerojet-General, Westinghouse Astronuclear Laboratory, and the Oak Ridge Y-12 Plant of Union Carbide Nuclear Company entered the program in the early 1960's, and their activities paralleled those of LASL in fuel element development.

## I. INTRODUCTION

Use of nuclear energy for propulsion was under study as early as 1946 when R. Serber, of Douglas Aircraft Company, published some fundamental considerations of the application of fission energy to rocket propulsion. Serber concluded that the most reasonable approach was conventional pile-heating coupled with a low-molecular-weight propellant and indicated that the improvement over chemical rockets would depend "entirely on how well the difficulties of heat transfer and high temperatures (material problems) can be solved."<sup>1</sup> How right he was! There were many other studies concerning use of nuclear energy for propulsion of rockets, ramjets, and other aircraft, including the well-known Nuclear Engine Propulsion Aircraft (NEPA) activities.<sup>2-7</sup> A comparison of a chemically powered Atlas missile

and a two-stage nuclear and chemical rocket system indicated a weight saving of  $\sim 50\%$  for the latter system with the same payload or, put another way, a doubled payload. Nuclear rocket propulsion, according to the calculations, could out-perform chemical propulsion in long-range, high-payload applications, if the nuclear system functioned as predicted. The best chemical rockets have a specific impulse of  $\sim 400$  s, whereas that of the nuclear rocket with hydrogen propellant is 900 s or more (see Fig. 1). Specific impulse is defined as the exhaust velocity divided by the acceleration of gravity ( $9.81 \text{ m/s}^2$ ).

The basic nuclear rocket engine concept is very simple. It consists of a nuclear reactor (Fig. 2) used to heat a low-molecular-weight gas (hydrogen) to as high a temperature as possible, a nozzle through which the gas expands, and a turbopump to force it through the system. The actual engine, of course, is

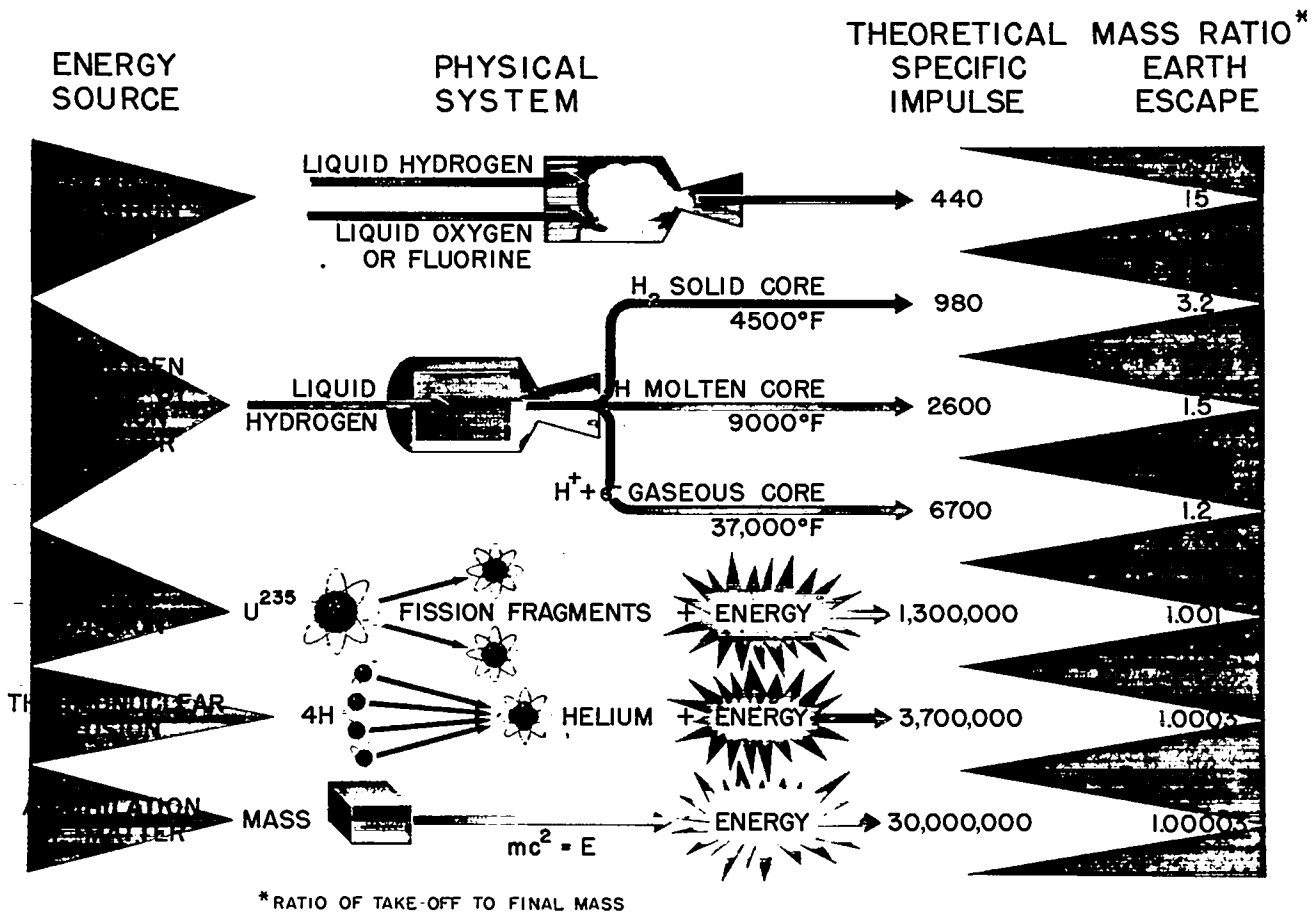


Fig. 1.  
Energy source vs specific impulse.

much more complicated. The reactors must operate at very high temperatures and power densities to minimize the effect of their weight. This combination of high temperature and high power density presented a real challenge to reactor designers and materials researchers.

Only a few materials, including the refractory metals and graphite, are suitable for use in reactors designed to run at very high temperatures. The metals are all strong neutron absorbers, whereas graphite is not. In fact, graphite, in addition to having excellent high-temperature strength, also acts as a neutron moderator and minimizes the amount of enriched uranium required in the reactor core. One great disadvantage of graphite, however, is that it reacts with hot hydrogen to form gaseous hydrocarbons and, unless protected, quickly erodes away. Consequently, one of the greatest challenges in the nuclear rocket program was to develop fuel elements of adequate lifetime in a high-pressure, hot hydrogen environment.

Temperatures above 2773 K (2500°C) were considered for fuel elements and exhaust gases, but little information on the behavior and compatibility of materials at these very high temperatures was available. Consequently, much work had to be done to gain a complete understanding of the behavior of materials in a nuclear rocket engine.

The Los Alamos Scientific Laboratory (LASL) and the now Lawrence Livermore Laboratory (LLL) had been evaluating nuclear propulsion possibilities, and in 1955 both started active work on all aspects of a nuclear propulsion rocket system.<sup>8,9</sup> Uranium-loaded graphite was the proposed fuel element material, but each laboratory took a different approach to incorporating the uranium into the graphite. LLL worked extensively on impregnating commercial graphites with a liquid, uranium-bearing material, uranyl nitrate hexahydrate. It was possible to drive the liquid into the graphite pores and then bake the impregnated graphite, causing uranium oxide to remain within it. Subsequent

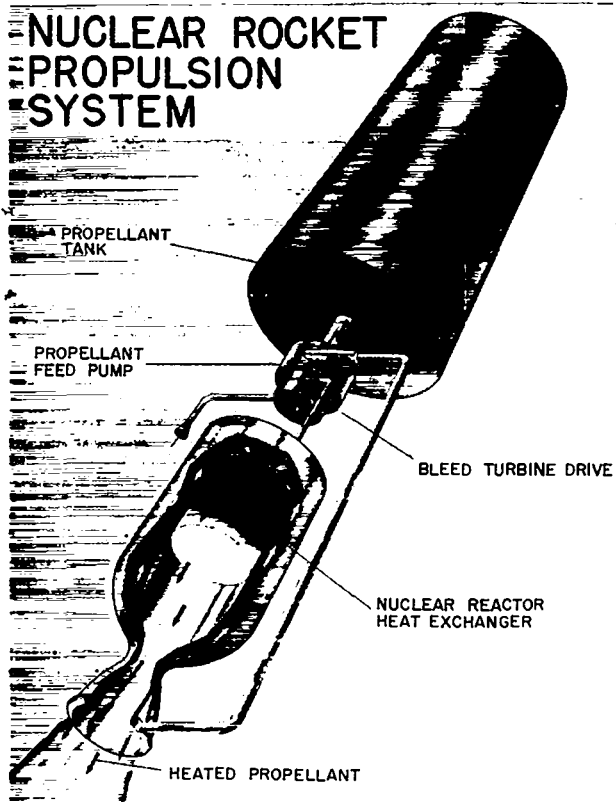


Fig. 2.  
Nuclear rocket propulsion system.

heating to high temperatures converted the uranium oxide to uranium dicarbide. The problem was the graphite—it was not uniformly porous, so the uranium oxide was not distributed uniformly. A program for developing a well-defined, porous graphite with interconnecting pores would be required to permit use of impregnation. At this point, LLL turned from rocket propulsion to an aircraft propulsion system, Pluto, that required an air-breathing rocket and different fuel materials.

LASL worked to incorporate  $UO_2$  particles into graphite fuel element matrices. This involved actual fabrication of a graphite body rather than purchase of commercial graphite. Consequently, LASL had to develop an entirely new (for them) technology to produce a fuel element material with very uniform distribution of micron-size uranium particles and adequate strength, stability, and corrosion resistance to operate at temperatures as high as 2773 K (2500°C) in a hydrogen environment. From 1955 to 1972, a very extensive uranium-loaded graphite fuel element technology evolved. This report can only be an overview of its development, because the total effort in fuel element technology, including ex-

trusion, coating, evaluation, nondestructive testing (NDT), etc. would, and does, fill many volumes.

At LASL, the nuclear rocket work was known as the Rover program throughout its history. It began in 1955 with AEC sponsorship, and, at LASL, was directed first by R. E. Schreiber and later by R. W. Spence. In 1960, the Space Nuclear Propulsion Office (SNPO) in Washington, DC, was created to manage the nuclear propulsion effort. Harold F. Finger headed the agency, which reported to both the AEC and the National Aeronautics and Space Administration (NASA). In 1961, the industrial team of Aerojet-General and the Westinghouse Electric Company was selected to develop the flight engine, and the nuclear engine for rocket propulsion application (NERVA) acronym was introduced. LASL continued to work on materials development and reactor design.

In 1962, the engine test site at Jackass Flats in Nevada was separated administratively from nuclear weapons activity and became the Nuclear Rocket Development Station (NRDS). During the existence of NRDS, 6 NERVA nuclear engines and 13 LASL reactors, ranging from the first 7-MW KIWI-A reactor to the >4000-MW Phoebus 2A reactor, were tested. All told, over 6 000 000 kWh of power were produced there. The Appendix summarizes the reactor tests performed at NRDS. Figure 3 shows the test cell with its large hydrogen Dewars.

## II. REACTOR DESIGN

The designers of the NERVA engine had to consider many factors, such as neutronics, heat transfer requirements, high mechanical loadings, and the complex problems of start-up, control, and shut-down. To permit preliminary evaluation of the neutronic calculations, for each type of reactor, a mockup known as Honeycomb (Fig. 4), which it resembled, was made of graphite slabs, enriched uranium foils, plastics to simulate propellants, and beryllium reflector blocks. Later, during construction of each new type of reactor, a more exact mockup of the final reactor core, known as Zepo (Fig. 5), was built using actual fuel elements to determine the system neutronics (Fig. 6). Honeycomb, and Zepo in particular, were important facets of each reactor design, and a separate set of fuel elements had to be fabricated for Zepo in each instance. LASL-designed reactors were tested at LASL, and similar facilities were available at Westinghouse Astronuclear Laboratory (WANL). The actual reactor and engine tests were carried out at NRDS.

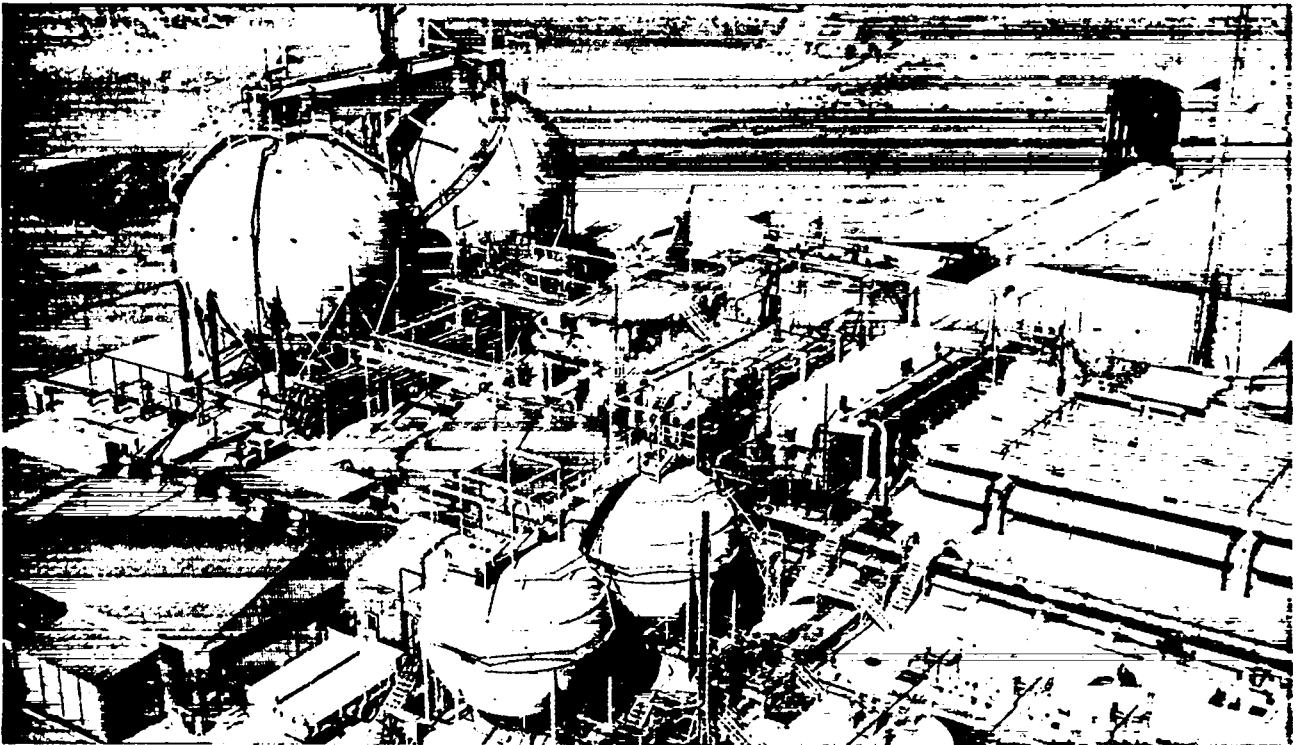


Fig. 3.  
Hydrogen Dewars and reactor test cell at NRDS.

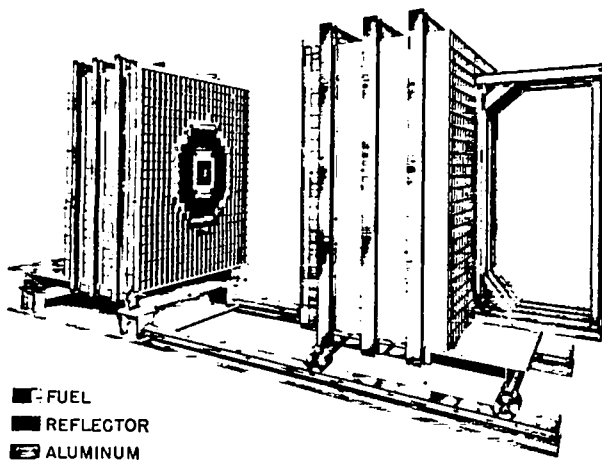


Fig. 4.  
Honeycomb assembly machine.

While the fuel and components for a specific reactor were being fabricated, the design engineers worked on the next reactor concept so that there was no lag in either design or fabrication. One of the

accepted disadvantages of this continuous activity was that feedback of reactor test results generally was too late for serious input into the next reactor test. However, changes could be incorporated into subsequent reactor designs.

The first Rover reactors were the 100-MW KIWI-As, named for the wingless, flightless bird of New Zealand. They were designed more as experiments to demonstrate proof of principle than as rocket engines, and they provided a significant amount of information. Next were KIWI-Bs, 1000-MW, 50 000-lb-thrust designs, that incorporated some of the features of a nuclear engine and provided invaluable experience in fabrication, coating, and testing of fuel elements. The Phoebus reactors were nuclear engine prototypes. Phoebus 1, designed for 1500 MW and 75 000-lb thrust, had an 889-mm (35-in.) -diam core, and Phoebus 2, designed for 5000 MW and 250 000-lb thrust, had a 1397-mm (55-in.) -diam core. The NERVA engines that WANL fielded were designated NRX-A and were comparable in size and thrust to Phoebus 1.

Later, LASL designed and built the Pewee reactor with a 508-mm (20-in.) -diam core for fuel element testing. It was a small version of Phoebus 1 which used  $ZrH_2$  rods as moderators in the core. Pewee

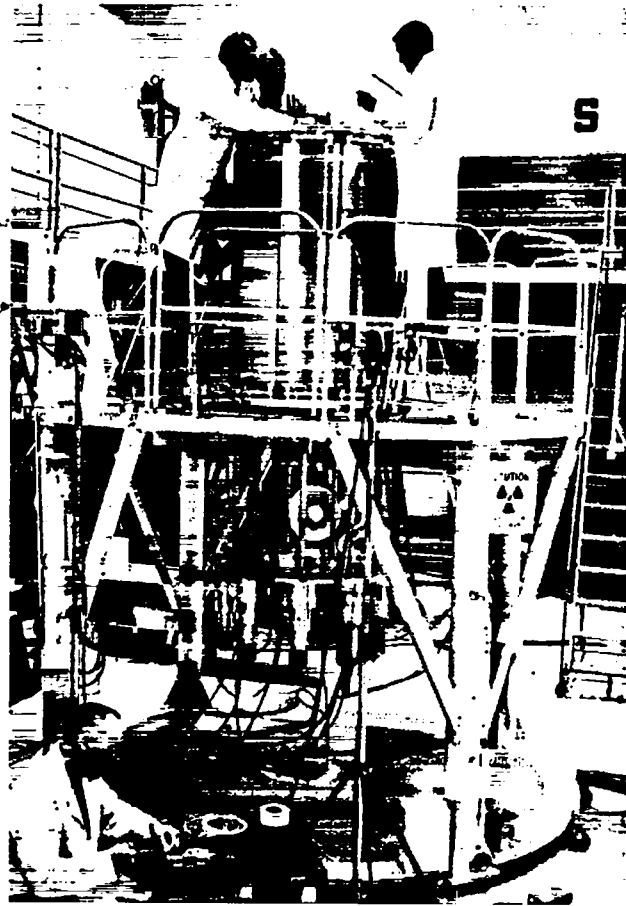


Fig. 5.  
Zepo assembly.

operated at the same power per fuel element as Phoebus 1 but required only about one-fourth as many fuel elements.

Finally, LASL designed and built the water-moderated Nuclear Furnace test reactor that provided reasonable simulation of full-scale reactor conditions for fuel element evaluation.

### III. KIWI-A

The first Rover reactor designed and built at LASL was called KIWI-A (Fig. 7), designed to produce ~100 MW. The design involved four whims of uranium-loaded graphite fuel plates and a fifth of unloaded graphite plates. A whim is a wheel-like structure with wedge-shaped boxes of fuel plates fitted between its spokes (Figs. 8 and 9). There were 12 boxes in each whim, and each box held 20 fuel plates. The uranium loading of each plate differed to provide a relatively flat radial fission distribution.

The plates were 190.5 mm (7.5 in.) long, 6.35 mm (0.250 in.) thick, and 123.2-200.7 mm (4.85-7.90 in.) wide, depending on their location in the wedge-shaped box. One face of each plate bore a series of longitudinal ribs that extended 1.27 mm (0.050 in.) above the plate surface to provide channels for the propellant gas.

The KIWI-A fuel plates were molded at room temperature in an evacuated die at 48.3 MPa (7000 psi). The binder for the filler components was a thermosetting resin, and the plates were cured slowly to polymerize the resin, impregnated with the same resin to increase their carbon density, cured, and then processed to 2723 K (2450°C). Only the one reactor with plate-type fuel elements was produced, and the technology was not representative of that developed for the nuclear rocket engine fuel elements.<sup>10</sup>

The fuel plates were specified to be radiographically sound and free of cracks, laminations, and voids. Carbon density was extremely important for neutronic reasons and had to be at least 1.70 Mg/m<sup>3</sup>. Compressive strength of at least 24.1 MPa (3500 psi) was required. The uranium distribution had to be uniform to within 5%, and the amount of uranium in each plate was specified in Megagrams per cubic meter of plate volume. This relationship tied the uranium loading to the carbon density, and this type of uranium density specification was used for all fuel elements in the Rover and NERVA program. The KIWI-A fuel plates were not clad or coated.

KIWI-A was tested in July 1959, ran for 300 s at 70 MW using gaseous hydrogen at 3.2 kg/s as the propellant, and provided important information on reactor design and materials. The fuel was hot enough to melt the carbide fuel particles. The UC<sub>2</sub>-carbon eutectic temperature is 2683 K (2410°C).

## IV. MATERIALS AND FABRICATION PROCEDURES

### A. KIWI-A Prime

KIWI-A prime was tested at NRDS about 1 yr later, on July 8, 1960. This reactor was designed to produce ~100 MW of power and to test a new core configuration. Instead of fuel plates, it had 19-mm (0.75-in.) -diam fuel cylinders, each containing four axial holes for propellant flow. The fuel elements were contained in ~1372-mm (54-in.) -long, high-density, commercial graphite modules (Fig. 10). The individual elements were 216 mm (8.5 in.) long, and six, one on top of another, made up the total fuel element length of ~1321 mm (51 in.). Each module held seven 51-in. elements.

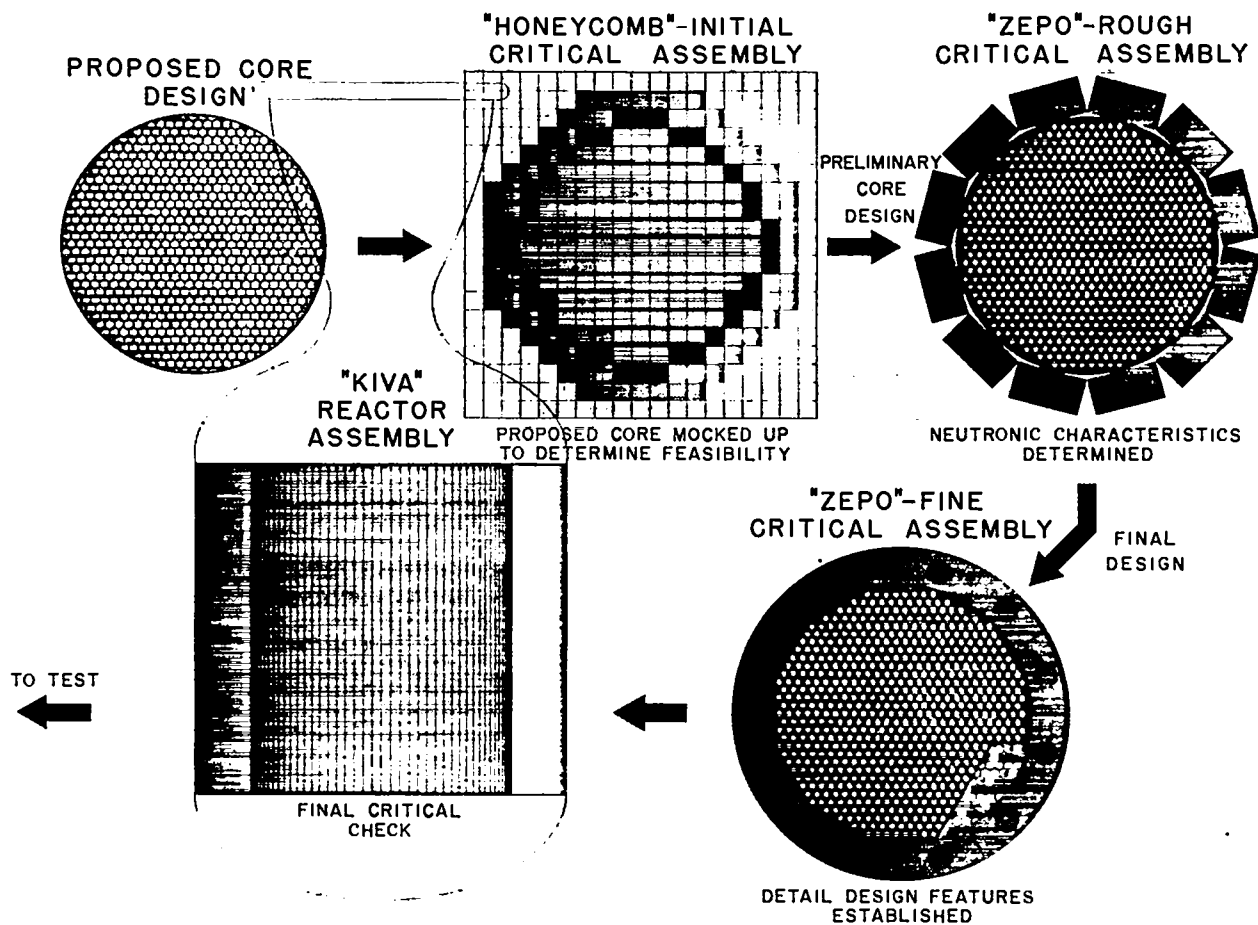


Fig. 6.  
Evaluation of neutronic design.

The KIWI-A prime fuel element introduced a major change in the fabrication process—we had to move from pressing and molding to a completely unknown graphite extrusion process. We invited Myron T. Cory, President of Graphite Specialties Corporation, Niagara Falls, NY, to serve as a consultant, in view of his extensive graphite extrusion experience. Myron helped us avoid many pitfalls over several years.

In describing the activities undertaken to produce fuel elements for the various designs of Rover and NERVA reactors, I will discuss primarily the LASL activities, with which I am most familiar, but similar development was under way at WANL and Oak Ridge Y-12. Excellent communication among the three facilities contributed to the progress in all areas of reactor and fuel element development. Where possible, I will attempt to acknowledge the individuals responsible for each area of work. At LASL, development of the pressed or extruded

uranium-loaded fuel element blank through its graphitized state for the entire Rover program is directly attributable to the dedicated work of Donald H. Schell. His competent and detailed work was the basis for the subsequent fuel element work at WANL and Oak Ridge Y-12. He deserves a large share of the credit for the fuel element technology developed in the Rover program. Joseph W. Taylor assisted in fuel element development and was responsible for production of all elements produced at LASL. He shares with Schell the credit for advanced fuel element technology. W. W. Martin and K. V. Davidson also participated in fuel element development and production.

The Oak Ridge Y-12 plant of Union Carbide Nuclear Corporation was brought into the Rover program when the need for large numbers of reactor fuel elements was anticipated and LASL would require help in supplying elements for specific reactors while still carrying on its fuel element development

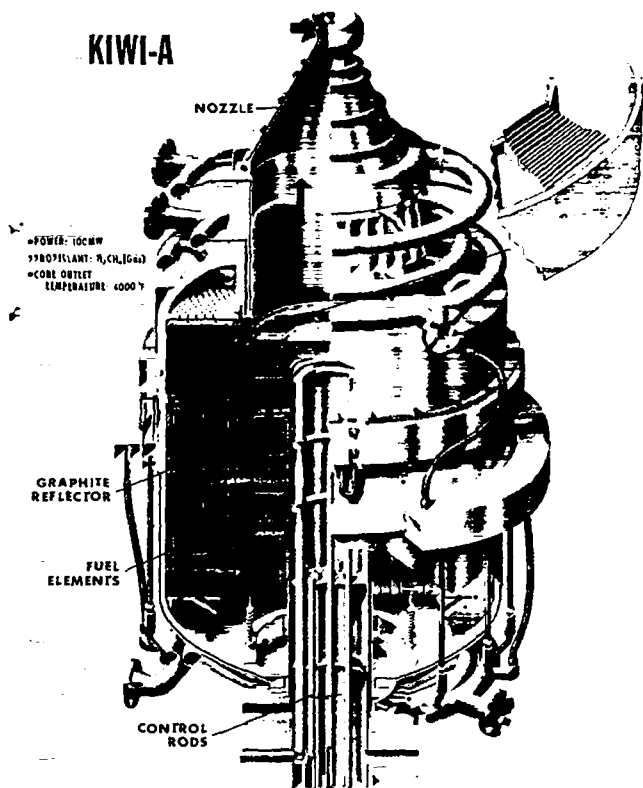


Fig. 7.  
KIWI-A reactor.

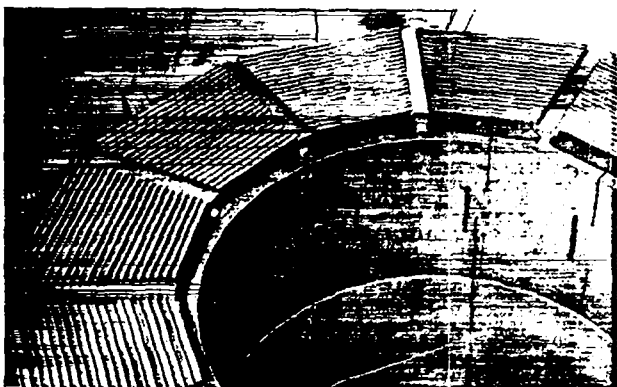


Fig. 8.  
Graphite whim with fuel plates.

work. The basic LASL technology for coated fuel element fabrication was transferred to Y-12 as a starting point for their participation. F. M. Tench headed the Y-12 effort, and the extrusion, graphitization, and coating were the direct responsibility of John M. Napier.

WANL was responsible for the nuclear components when NERVA was introduced in 1961, and their overall effort paralleled that of LASL. The WANL development activities were under the general direction of A. Boltax; Ronald Cost and Robert Eichinger were responsible for fuel element extrusion.

## B. Types of Fuel Particles

The major changes made in the basic fuel elements, other than those in geometry, were in the type of enriched uranium fuel incorporated into the graphite matrix. The fuel particle in all of the KIWI-A reactors and those through KIWI-B4D in the KIWI-B series was highly enriched  $UO_2$ . KIWI-B4E, Phoebus 1, Phoebus 2, Pewee, and NRX-A, tested from 1964 through 1969, all incorporated "beaded" particles, highly enriched  $UC_2$  cores coated with pyrolytic graphite. Nuclear Furnace (NF-1), operated in 1972, tested two new LASL fuel element loading concepts. The first was a small, pure carbide (U,Zr)C (no graphite) element capable of withstanding very high temperature. The so-called "composite" fuel element was a 19-hole, hexagonal design in which the fuel was uncoated (U,Zr)C particles, the total carbide loading was 35 vol%, and the uranium content was varied as required. Discussion of fuel element technology, therefore, will focus on the  $UO_2$  and coated-particle loaded fuel elements, with some review of the more advanced and very promising composite element technology.

## C. Typical Processing Equipment

LASL obtained a 150-ton Elmes hydraulic extrusion press that could maintain constant extrusion speed even if extrusion pressure varied. The available extrusion cylinders for the press were 457 mm (18 in.) long and 63.5-203 mm (2.5-8 in.) in diameter. We designed the accessories that we considered essential for extrusion of high-quality fuel elements. A vacuum pump with a cold trap was designed so that the cylinder containing the green (uncured) mix could be evacuated before extrusion. Air trapped within extruded fuel elements expanded during subsequent heat treatments, creating unacceptable porosity and cracks. The press ram, etc. had to be modified to permit the vacuum outgassing.

Graphite fixtures and a special run-out table to hold them (Fig. 11) were designed and built at LASL so that the weak, green fuel elements were extruded

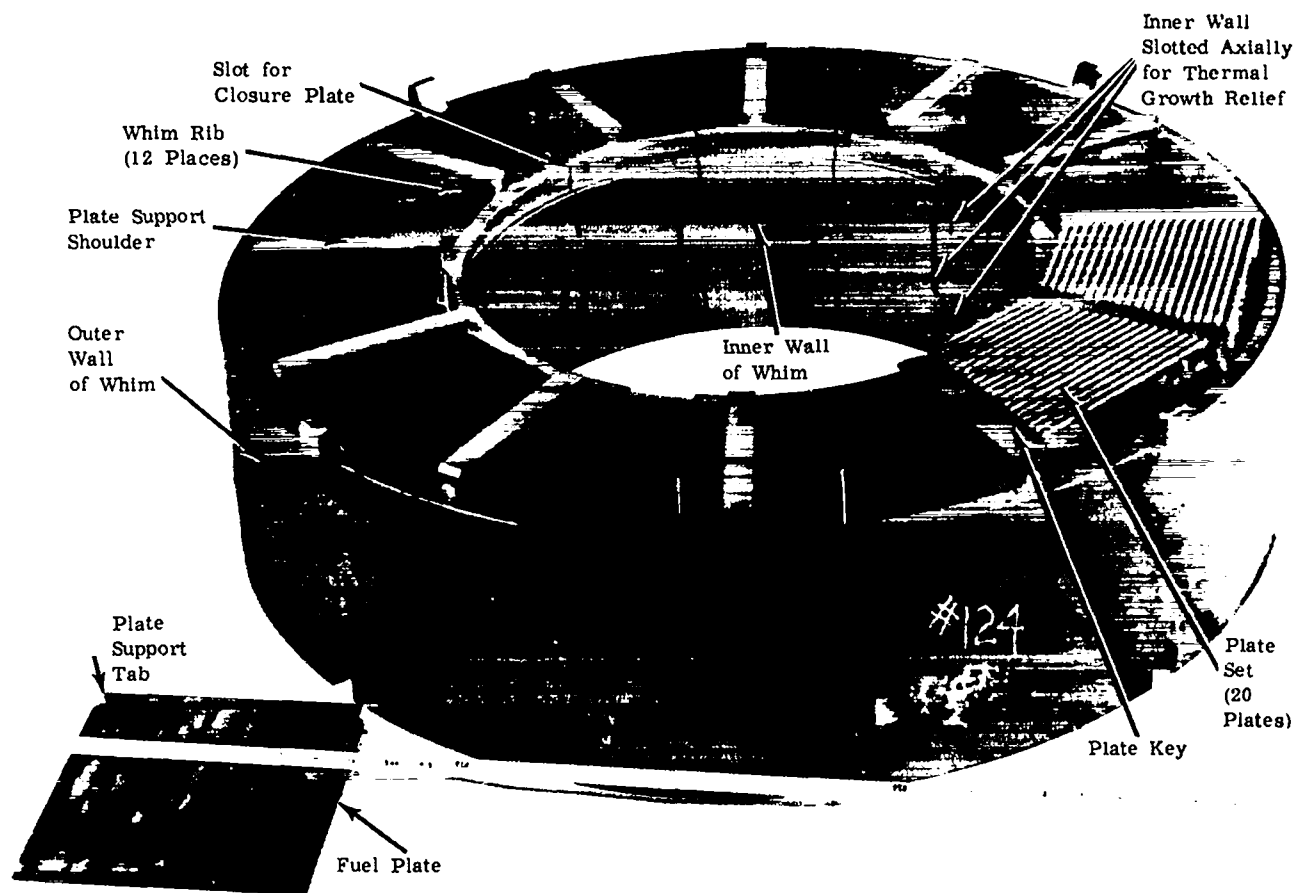


Fig. 9.  
Fifth whim during assembly.

directly into the fixtures which were then used in the curing ovens. Ovens and furnaces for the necessary heating operations were either purchased or designed and built at LASL. The electric ovens all had cam-controlled temperature controllers so that a rise as slow as 1 K/h ( $1^{\circ}\text{C}/\text{h}$ ) could be programmed over critical ranges. The high-temperature graphitizing furnaces were induction heated by 175-kW, 960-Hz generators, temperatures were read with optical pyrometers, and the power was controlled manually.

#### D. Raw Materials

The dry carbon in the early extrusion mixes was 77.5 wt% graphite flour, 7.5 wt% flake graphite, and 15 wt% carbon black. Later, the flake graphite was eliminated and the composition became 85 wt% graphite flour and 15 wt% carbon black.

1. **Graphite Flour.** The primary filler in the extrusion mix was graphite flour. This material was selected because it was readily available, relatively cheap, and reasonably pure and, because it had been at graphitizing temperatures, shrank little, and had relatively high particle density. The resulting extruded product shrank little during processing and had high carbon density, good dimensional stability, and relatively high thermal conductivity. The graphite flour was made from specially selected and ground scrap commercial electrodes (made from soft coke base) that had been impregnated to give a minimum density of  $1.65 \text{ Mg}/\text{m}^3$ . The particles were isotropic and nonneedle-like in appearance. This material, Graphite Flour No. 1008, was obtained from the Great Lakes Carbon Company, Niagara Falls, NY. A typical particle size analysis of the flour used for all  $\text{UO}_2$ -loaded fuel elements showed it to be 100% -35 mesh, as follows.

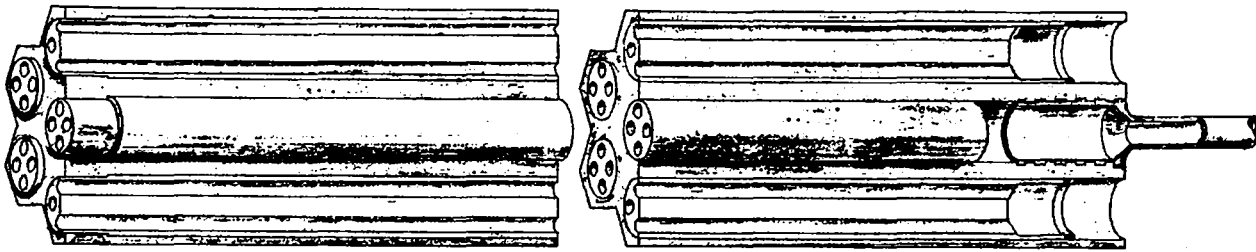


Fig. 10.  
Fuel elements in graphite module.

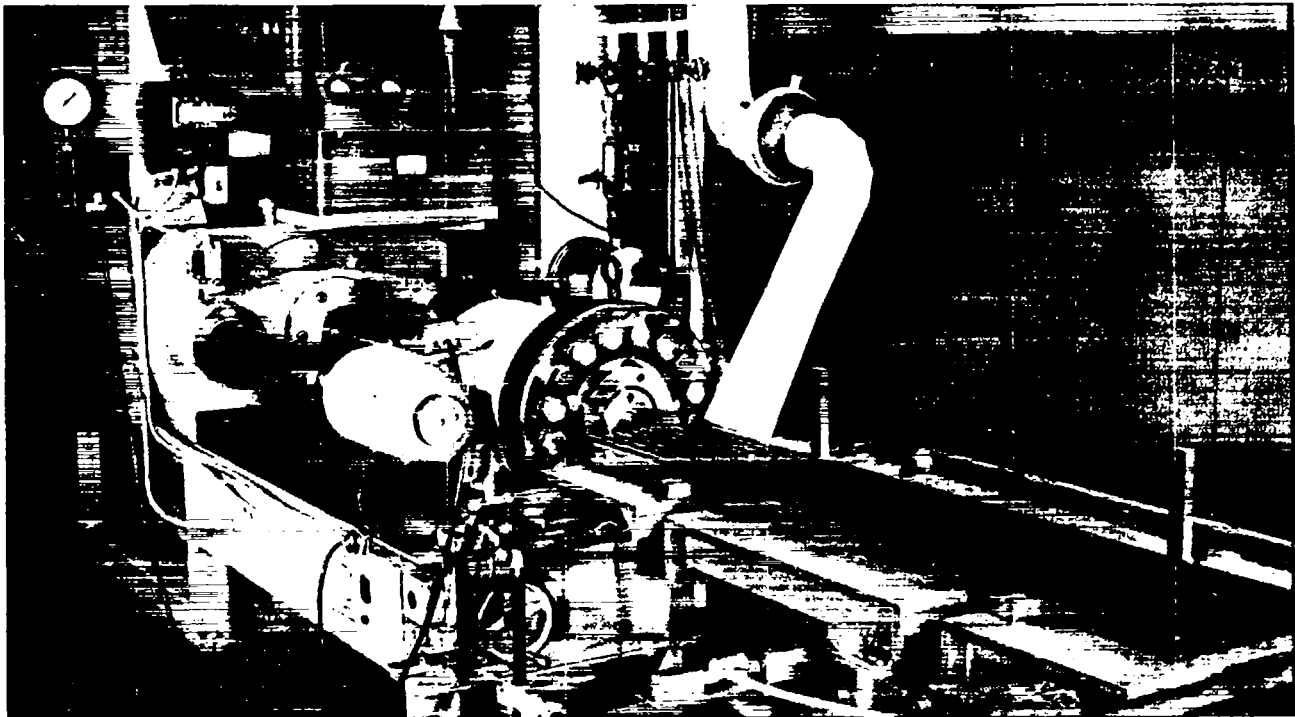


Fig. 11.  
Fuel element extrusion press and fixture table.

2%	- 35	+100
20%	-100	+150
20%	-150	+200
15%	-200	+270
10%	-270	+325
33%	-325	mesh

When beads (coated  $UC_2$  particles) were introduced to replace  $UO_2$  as the fuel, the particle size specification was changed so that ~70% of the graphite flour was -325 mesh. This type of flour was also used for the composite fuel elements developed later.

The average particle size of the -325 mesh fraction as measured on a Fisher Sub-Sieve Sizer was  $3.4 \mu\text{m}$ . The flour had a helium density of  $2.12 \text{ Mg/m}^3$  and a surface area of  $3.9 \text{ m}^2/\text{g}$ .

The No. 1008 flour was shipped in steel barrels, each containing  $\sim 136 \text{ kg}$ . There was an indication that extrusions made from the flour near the bottom of a barrel contained more high-density impurity inclusions than normal. Possibly, during shipping and handling, high-density impurities in the flour tended to settle. Therefore, we used only the flour in the top three-quarters of each barrel.

The flour was passed over a magnetic separator, and that from several barrels was cross-blended to give a large uniform quantity for blending with the other carbon ingredients. The material collected on the magnets was 41.5% iron and 4% silicon plus carbon. The flour had  $\sim 0.3\%$  ash content, the primary metallic constituent being iron with lesser amounts of silicon and calcium.

The original supply of No. 1008 graphite flour was eventually exhausted, and we bought another 9000-kg batch. This material was very similar to the original batch, and it had been ground carefully in an attempt to exclude all extraneous impurities, especially nonmetallics. However, the grinding plant was not set up to provide the quality control that we felt necessary. A number of problems in the graphitized elements could be traced back to impurities in the graphite flour.

In the large batches of graphite flour purchased later, the iron content was limited to a maximum of 100 ppm, silicon to 150 ppm, and boron to 3 ppm. These flours were designated M1, M2, etc., as they were obtained from Great Lakes Carbon Company, Morgantown, PA. The finer powder (70% -325 mesh) was also a high-purity material, designated S97 and obtained from Speer Graphite Company. The availability of high-purity flours and of graphite furnace fixtures made from purified (low-iron) graphite stock eliminated some of the problems that had been caused by low-melting impurities in the graphite.

**2. Carbon Black.** The carbon black used throughout the LASL program was a high-fired, low-shrinkage material called Thermax, a product of the Theratomic Carbon Company, Sterlington, LA. It was screened through a 60-mesh screen to break up large agglomerates, but varied from shipment to shipment in its ability to pass through the screen. At times, only 10% would pass through, whereas at other times 50% would pass. The amount of material passing through the screen could be in-

creased from 20 to 50% by heating the bagged Thermax at  $363 \text{ K}(90^\circ\text{C})$  for 16 h.

Thermax had an average particle size of  $\sim 0.9 \mu\text{m}$  as measured on a Fisher Sub-Sieve Sizer, and an almost spherical particle shape as shown by the electron microscope. The ash content was  $<0.15\%$ . Adding Thermax to the extrusion mix produced denser extrusions, apparently by filling the voids between large graphite particles thus increasing the packing density of the mix.

**3. Flake Graphite.** Adding a small amount of fine flake graphite to the pressing and extrusion mixes improved the product density. A synthetic graphite flake called BMG-D, a product of the Grafo Colloids Corp., Sharon, PA, was used for all flake additions. The flake was passed through a 60-mesh screen to break up any lumps and remove large flakes. Five per cent of the material was retained on the screen. BMG-D had an average particle size of  $1.8 \mu\text{m}$  as measured on a Fisher Sub-Sieve Sizer, and 0.8-1.5% ash content. The primary metallic constituent of the ash was iron. The BMG-D helium density was  $2.10 \text{ Mg/m}^3$ , and the surface area was  $32.0 \text{ m}^2/\text{g}$ .

**4. Uranium Dioxide.** The uranium loading in the form of highly enriched  $\text{UO}_2$  powder was added to the extrusion mix for the KIWI-A and -B type fuel elements by admixture. The  $\text{UO}_2$  was prepared within the Laboratory.<sup>11</sup> The conversion figure for uranium content of the oxide was 0.8781, indicating that 87.81 wt% was uranium. This approximated the oxygen content of  $\text{UO}_{2.04}$ .

The  $\text{UO}_2$  product was a relatively free-flowing, dense powder with up to 0.2 wt% +325-mesh, about 10 to 20 wt%  $>10\text{-}\mu\text{m}$ , and 5 to 10 wt%  $<2\text{-}\mu\text{m}$ , particles. The average particle size determined with a Fisher Sub-Sieve Sizer was  $\sim 4.5 \mu\text{m}$ . Particle density was shown to be  $\sim 10.9 \text{ Mg/m}^3$  by helium displacement; loose bulk density,  $\sim 4 \text{ Mg/m}^3$ . The principal impurity was 200 to 2000 ppm of iron. Chromium content was usually below 50 ppm.

Quality control consisted of the following analyses on each unit of a final cross-blended batch: isotopic, spectrographic uranium assay, gamma activity, loose bulk density, and sieving to determine the amount of +325-mesh powder. Particle size distribution of a sample from the final cross-blended batch was also measured.

All development work for preparation of the enriched oxide was done with oxide made from depleted uranium. WANL and Oak Ridge Y-12 obtained the enriched  $\text{UO}_2$  used in their fuel elements from commercial suppliers.

TABLE I

## RESULTS OF ROUTINE LASL QUALITY EVALUATION OF COATED PARTICLES FROM GENERAL ATOMIC PRODUCTION LOT GA-E-LY-121

Property	Value
Uranium Content (wt%)	68.22
Oxygen content (ppm)	105 - 210
Nitrogen content (ppm)	200
Spec impurities (ppm)	
Iron	24
Silicon	2
Boron	0.2
Other >25	---
Uranium leached (% of total)	0.02
Particle size distribution	0.0
(< + 208 $\mu\text{m}$ )	0.0
(147 - 208 $\mu\text{m}$ )	54.4
(88 - 147 $\mu\text{m}$ )	45.5
(-88 $\mu\text{m}$ )	0.1
Particle density ( $\text{Mg}/\text{m}^3$ )	4.85
Calculated uranium density ( $\text{Mg}/\text{m}^3$ )	3.31
Coating density ( $\text{Mg}/\text{in}^3$ )	1.80
Thermal stability at 2573 K (2300°C) for 4 h	
Penetrated coatings (%)	0
$\geq 5 \mu\text{m}$ of unattacked coating (%)	100
$\geq 10 \mu\text{m}$ of unattacked coating (%)	99

The crushing strength of typical coated particles was  $\sim 0.4$  kg/particle.

**5. Coated  $\text{UC}_2$  Particles.** The first work of any magnitude on coated particles of uranium compounds probably was performed by the British in developing fuel for their Dragon gas-cooled reactor. In the U.S., the 3M, Carbon Products Division of Union Carbide Corp., and General Atomic (GA) companies did extensive work on pyrolytic carbon and graphite coating of  $\text{UC}_2$  particles, which became available on a routine production basis in 1964. GA continued their development program because of their interest and participation in the high-temperature gas reactor (HTGR) concept. The beads (coated particles) used for fuel element development and fabrication at LASL, WANL, and Y-12 were mostly from GA, although KIWI-B4E, the first core with bead-loaded fuel elements, used 3M beads. GA coated particle development was directed by J. C. Bokros and W. Goeddel.<sup>12</sup>

During this time, LASL was doing very extensive research and development work on improved (higher temperature capability) coated particles under the direction of Richard J. Bard.<sup>13,14</sup> The coated particles were used *not* for their fission product retention, the principal requirement in conventional nuclear power reactors, but to protect the  $\text{UC}_2$  particles against oxidation and reaction with coating gases during fuel element fabrication and storage. The early protective coatings had only a low-temperature (for Rover) capability and undoubtedly were destroyed or damaged during the high-temperature reactor tests.

The size of the coated particles used in 19-hole fuel elements was restricted by the relatively thin (0.76-mm) web between holes. The 50- to 150- $\mu\text{m}$ -diam  $\text{UC}_2$  core coated with a nominal 25- $\mu\text{m}$ -thick pyrocarbon coat could go through the rigorous fuel element fabrication process with a relatively small percentage of damaged particles. This, therefore was the coated particle size used in most fuel elements.

The coated particles received at LASL were evaluated before being released for fuel element fabrication. A typical evaluation that met LASL specification, CMB-8-3819, is shown in Table I.

**6. Thermosetting Resin.** Varcum 8251 thermosetting resin was selected as the most satisfactory binder for the graphite flour and fuel particle extrusion mix. Various phenolic resins, some available as powder or liquid, also revealed good coking (carbon residue) values. The extrusions made with phenolic resins were much more brittle than those made using Varcum, so they were eliminated from consideration. Varcum is a partially polymerized furfuryl alcohol prepared by the Varcum Chemical Division of Reichold, Inc., Niagara Falls, NY. Varcum viscosity varied from shipment to ship-

ment but averaged 0.3-0.4 Pa·s. One complete processing batch of Varcum was prepared for the LASL order, and the vendor cross-blended all the drums of material from the batch to ensure as much uniformity as possible. The useful shelf life of the uncatalyzed resin in low-temperature storage was several months, although the viscosity did increase somewhat with time. The density was  $\sim 1.20 \text{ Mg}/\text{m}^3$ , and the nominal carbon yield was 45%. The carbon produced from Varcum was considered a "glassy" carbon and it was difficult to graphitize even at high temperatures. The Varcum for each day's use was catalyzed that day.

**7. Catalyst.** Varcum was catalyzed with 0.04 kg of maleic anhydride per kilogram of resin. The anhydride was ground into powder, using a mortar and pestle, and screened through a 20-mesh screen. The powder was added to the resin, and the mixture was stirred vigorously with a laboratory stirrer for 20 min to dissolve the catalyst. This amount of catalyst was slow acting at 313 K (40°C), so processing times were not sensitive. The flour and binder mixtures were usable after several days' storage at room temperature and even after several weeks' storage at 275 K (2°C).

## E. Blending and Extrusion

The KIWI-A prime fuel elements were extruded as nominally 25.4-mm (1-in.) -diam tubes each containing four axial holes.<sup>15</sup> The dry carbon in the extrusion mix was 77.5 wt% graphite flour, 15 wt% carbon black, and 7.5 wt% flake graphite. The uranium loading of highly enriched  $UO_2$  powder was added to this mix. The extrusion mix was bonded with Varcum amounting to 29% of the combined weight of the dry carbon ingredients plus 25% of the  $UO_2$  weight. This total composition evolved from extensive development which indicated that this resin content with 15 wt% carbon black gave the densest fuel elements. Because carbon density was extremely important to the system neutronics, this composition was used for most Rover fuel elements.

The dry carbon ingredients were blended first in 50-kg batches. One-kg amounts were taken from the large batch and put in glass containers, the  $UO_2$  was added, and the jars were rolled to homogenize the mixtures. The catalyzed resin was then hand-mixed with the graphite and  $UO_2$  blend to prepare it for extrusion. We soon improved upon this procedure by using twin-shell P-K blenders with intensifier bars (Fig. 12) that mixed the carbon,  $UO_2$ , and resin in one operation. This became standard mixing procedure for all fuel elements.

The blended mix was then fed through a commercial meat grinder (Fig. 13) one or more times to homogenize it further. This product became the feed for the extrusion press; the 203-mm (8-in.) -diam extrusion cylinders would hold  $\sim 10$  kg of mix. The mix was extruded at 17.2 MPa (2500 psi) at  $\sim 0.03$  m/s, Fig. 14. The extruded product was run through the grinder again and reextruded two to four times, depending on the fuel particle type, fuel element



Fig. 12.  
P-K blender with extrusion mix.

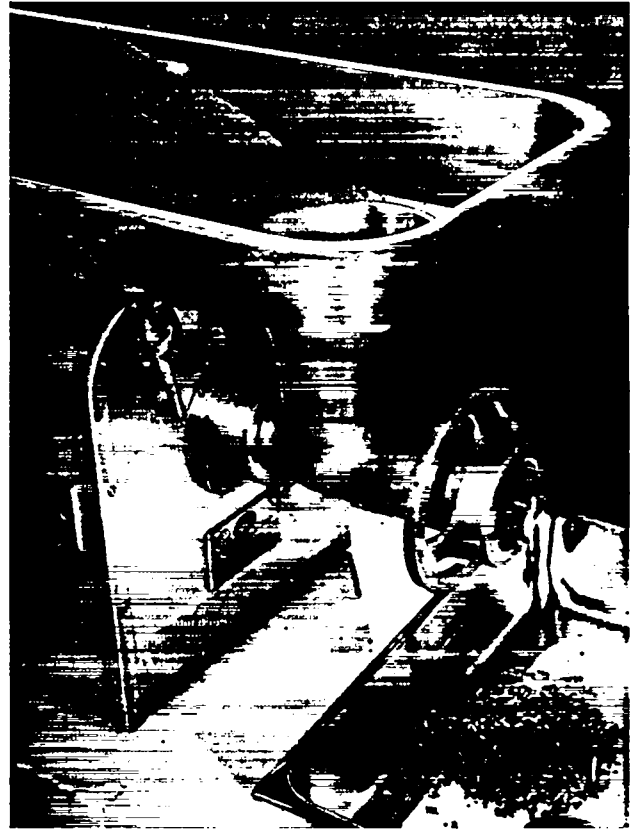


Fig. 13.  
Grinder and product.

geometry, and extrusion behavior. Repeating the extrusion operation in this way served as a homogenizing and densifying step.

The KIWI-A prime elements were extruded into 762-mm (30-in.) -long brass tubes. When the extrusion reached the end of the tube, the tube was lifted abruptly to break the extrusion at the die exit. The filled tube was removed and replaced with an empty one. The filled tube was placed in a semicylindrical groove in a graphite curing fixture and was pulled from around the extrusion, permitting it to rest in the graphite groove. This had to be done very carefully because the green extrusions were very plastic and required complete support. Serial numbers were scribed on each element as it lay in the fixture. The exact fuel element geometry was machined from the graphitized stock supplied to the machine shop.

The four-hole fuel element gave way to the 19-mm (0.75-in.) -diam, seven-hole extrusion for the KIWI-B1A reactor, and improvements were made as we became more experienced in extrusion. Development of extrusion dies to give the desired fuel element geometry and extrusion quality continued during the entire program. The major extrusion process

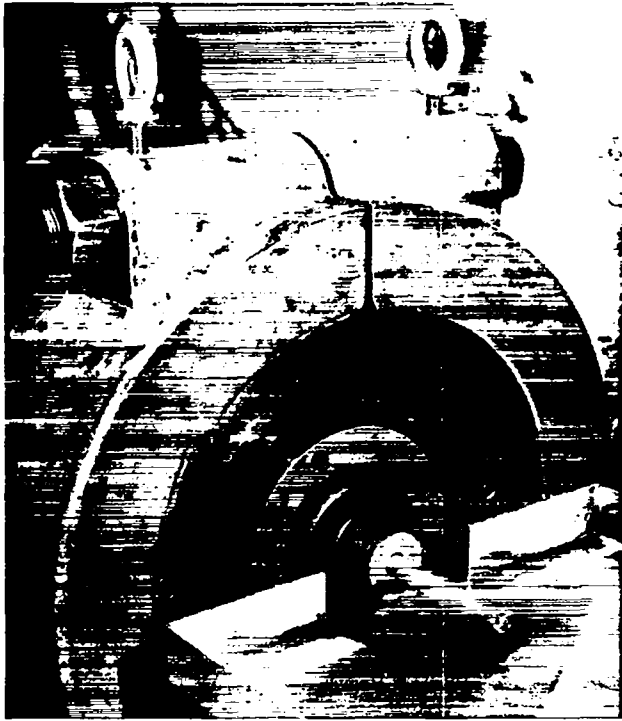


Fig. 14.

*Extrusion of KIWI-A prime four-hole fuel element.*

change occurred when the reactor designers called for a hexagonal element containing 37 small propellant holes running the length of the element. This required a much better understanding of material flow patterns through the extrusion die, and we built a 37-hole die based on our best ideas about material flow at that time. The die worked reasonably well, and we did produce a 37-hole hexagonal extrusion, indicating that reactor designers could consider such a fuel element concept seriously.

Fortunately, for other reasons, the designers decided on a 19-hole hexagonal fuel element with a flat-to-flat dimension of  $\sim 19$  mm (0.75 in.). The nominal diameter of each borehole was  $\sim 2.54$  mm (0.100 in.). Further, KIWI-B4 called for a one-piece fuel element  $\sim 1321$  mm (52 in.) long. This became the basic graphite fuel element design throughout the Rover program. The NERVA design in all of the WANL NRX-A reactors used the same basic fuel element (Fig. 15) as the Rover reactors.

The specifications for the 19-hole hexagonal element extrusion were not easy to meet. The holes were 2.36 mm (0.093 in.) in diameter, and each had to be within  $\pm 0.15$  mm (0.006 in.) of its true location to prevent localized overheating. The web thickness between interior holes was  $\sim 0.76$  mm (0.030 in.);

that between the outer row of holes and the outside of the element was somewhat less. The graphitized element could have a maximum twist of only 0.20 mm (0.008 in.) over its full length. Obviously, we went through many die design iterations to control hole location and maximize knitting of the extruded material where it flowed together around the pins that produced the holes. There was essentially no chance to correct hole position by later machining—the holes had to be extruded in the proper location! This meant that we were trying to produce a precision fuel element even in the green state. The extrusion material flow had to be controlled not only to locate the holes but also to provide enough turbulence and pressure to recombine the separated flows at the exit end of the die. Inadequate turbulence would create a plane of weakness between holes along the length of the element which would open up during subsequent heat treatment and be detected during NDT. Consequently, we made many changes in extrusion die design, but eventually evolved designs (Figs. 16 and 17) that produced 19-hole fuel elements that met all specifications. However, many of the day-to-day problems in fuel element extrusion were related more to variations in mix behavior than to the tooling. Variations in binder behavior, extrusion mix temperature, and humidity were sometimes so subtle that it was difficult to explain why one batch behaved poorly and other presumably identical batches extruded beautifully. A certain amount of “art,” as well as adequate technical know-how, is required to produce high-quality fuel element extrusions.<sup>16</sup>

The 19-hole hexagonal elements were extruded directly into a 1625-mm (64-in.)-long machined graphite fixture precisely positioned so that the green element did not bend on emerging into it from the extrusion die, Fig. 18. The fixture was precisely machined so that each groove was three-sided (half a hexagon) with dimensions  $\sim 0.13$  mm (0.005 in.) larger than the extrusion. The extra length of the fixture provided room for fuel element shrinkage during the subsequent heat treatment as well as for trimming the element ends to remove short lengths that might have been distorted when the green extrusion was cut and the fixture moved over to the next element position. A cover plate with matching grooves was positioned over the fixture filled with green extrusions so that the fuel elements were completely contained.

We encountered one situation that illustrates the unexpected problems that can occur. The specifications called for a maximum 0.20-mm (0.008-in.) twist over the 1320-mm (52-in.) length of the element. The elements were extruded into

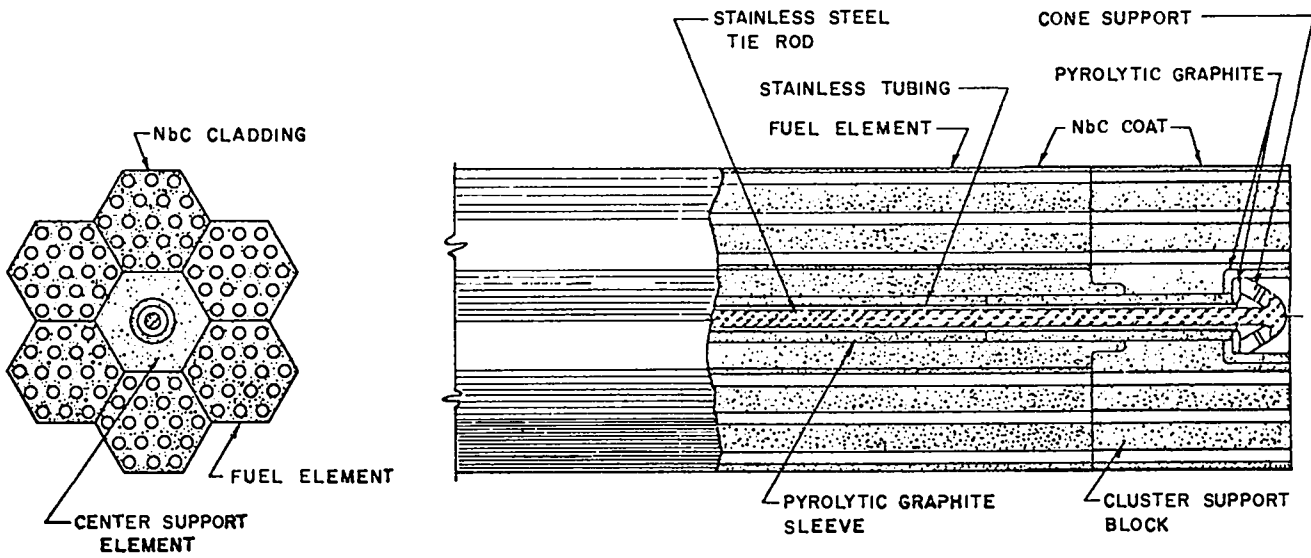
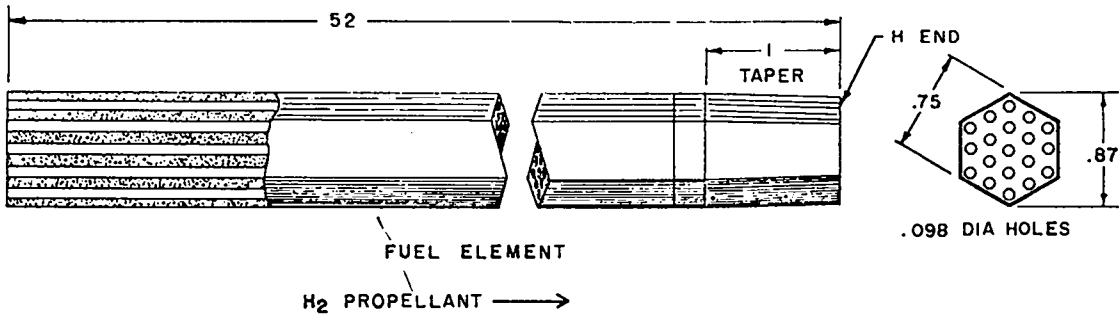


Fig. 15.  
Nineteen-hole fuel element and a fuel element cluster.

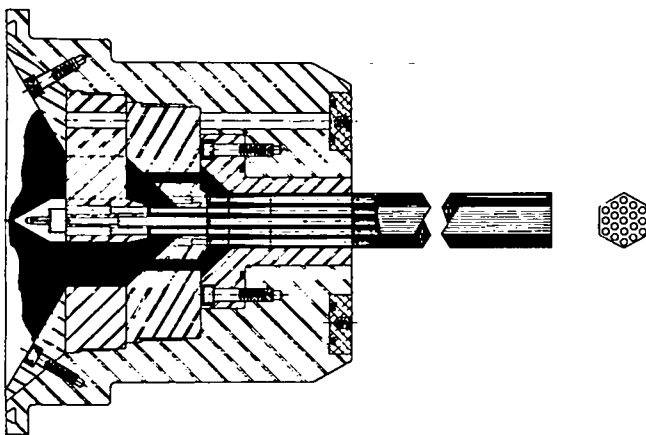


Fig. 16.  
Extrusion die and material flow.



Fig. 17.  
Extrusion die components for hexagonal, 19-hole fuel elements.

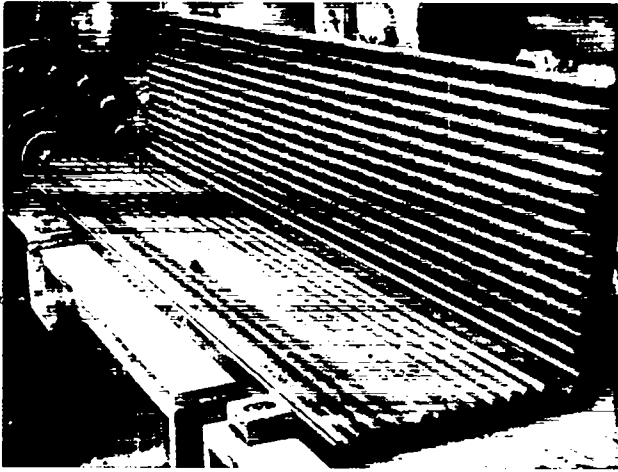


Fig. 18.

*Nineteen-hole fuel elements being extruded into graphite fixture. Graphite cover plate is at right.*

precision-machined fixtures and held in them during all heat treatments so that they should have been very straight. However, the hexagonal elements were seriously twisted after the early stages of heat treatment. After much effort in reviewing the straightness of fixtures, tolerances, procedures, etc., we discovered that the die plenum, which created the hexagonal outer shape of the element, was twisted 0.025-0.05 mm (1-2 mils) over its 50-mm (2-in.) length. The hexagonal shape had been machined into the steel plenum by electrodischarge machining, and the electrode had twisted while creating the hexagonal hole. The resin-bonded graphite had a plastic memory, and the element, during low-temperature polymerization of the resin, reverted to the twist it had been given during extrusion. Reducing the die twist to less than 0.013 mm (0.5 mil) eliminated the element twist. This problem warned us that the green element could not be distorted even slightly if we were to produce quality fuel elements.

## F. Heat Treatments

1. **KIWI-A through -B4D Oxide-Loaded Elements.** The first heat treatment was a low-temperature curing cycle to polymerize the thermosetting resin used as the binder. This was a very critical operation because of the large volumes of gas evolved and the potential for cracking the weak element. The total time to reach 523 K (250°C) was ~56 h, 12 h being required to go from 313 to 473 K (40-100°C) and another 15 h to go from 473 to 403 K

(100-130°C). After this low-temperature treatment, the fuel elements could be handled without support. The subsequent one or two oven treatments, to as high as 1123 K (850°C), were essentially outgassing steps to remove further gaseous products of the resin breakdown. Here again, there were certain critical temperature ranges through which the heating rate was extremely slow. The specific areas of critical temperature were determined by differential thermal analysis and thermogravimetric analysis of the resin binders and by observation of temperatures at which large volumes of gases evolved. The Rover fuel element geometry was favorable to use of resin binder because the webs between holes were thin and it was relatively easy for gases to escape. Where thicker cross sections of unfueled graphite were required, we added a low-temperature material such as wood flour to the extrusion mix. The wood flour burned out at relatively low temperatures, creating porosity that permitted the gases from resin decomposition to escape without building up pressure that would cause defects. Use of a resin binder for thick sections without holes may not give the same quality product.

We determined the shrinkage of each type (fuel loading) of element during each heat treatment. Each successive graphite fixture was sized to the fuel element dimension after the preceding heat treatment. The total volume shrinkage of the elements was ~15%, better than half of which occurred during the low-temperature heat treatment. In analyzing the hole location in thin wafers cut from the extruded element, each hole was inspected for its true location relative to its design location. We found that there were three different shrinkage patterns depending on the location of the hole in the element. This information had to be fed back into the die design data so that the pin location in the extrusion die would accommodate the various shrinkage patterns. The purpose of different fixtures, of course, was to keep the elements as straight as possible and to minimize excess room that would allow the element to distort as it shrank. The graphite fixtures themselves were very stable and did not distort during the heat treatment.

The final, so-called graphitizing, treatment was performed in induction-heated furnaces; the maximum temperature depended on the type of fuel particle in the element. Maximum temperature was easily achieved within 8 h, but 36-48 h were required to cool the element enough for removal from the furnace. The first graphitizing furnaces, Fig. 19, were designed to handle a 762-mm (30-in.)-long fuel element, and no serious attempts were made to control the furnace atmosphere. With the advent of the full-length element, new induction-heated furnaces



*Fig. 19.*  
*Early induction-heated graphitizing furnaces.*

(Fig. 20) were built, using a Micarta shell for the furnace wall. These furnaces could be evacuated and back-filled with dry helium to control their atmospheres throughout the heating cycle.

The maximum heat treatment temperature depended on the nature of the fuel particle incorporated into the element. The elements for KIWI-A through -B4D had  $UO_2$  fuel loading. From 1873 to 2273 K (1600-2000°C), the  $UO_2$  reacted with the carbon surrounding it and was converted to  $UC_2$  with evolution of CO and loss of carbon from the element.<sup>17</sup> Temperatures could go as high as the  $UC_2$ -C eutectic temperature, 2683 K (2410°C), at which the fuel melted. The major problem with oxide-loaded fuel elements was the so-called back-reaction. Micron-size  $UC_2$  particles are extremely reactive and revert to oxide in the presence of air, particularly humid air. Thus, oxide-carbide-oxide reactions occurred during each heating and storage cycle, including graphitizing, coating, and reactor operation, and each cycle caused loss of carbon by CO gas evolution and degraded the element. Dimensional changes also were noted in stored elements, and we had to change from plastic storage tubes, which were finitely water permeable, to metal tubes. Oxidation of the  $UC_2$  loading material caused the element to swell as much as 4% so that the final dimensions could not be controlled. An odor of acetylene gas accompanied the chemical reactions.

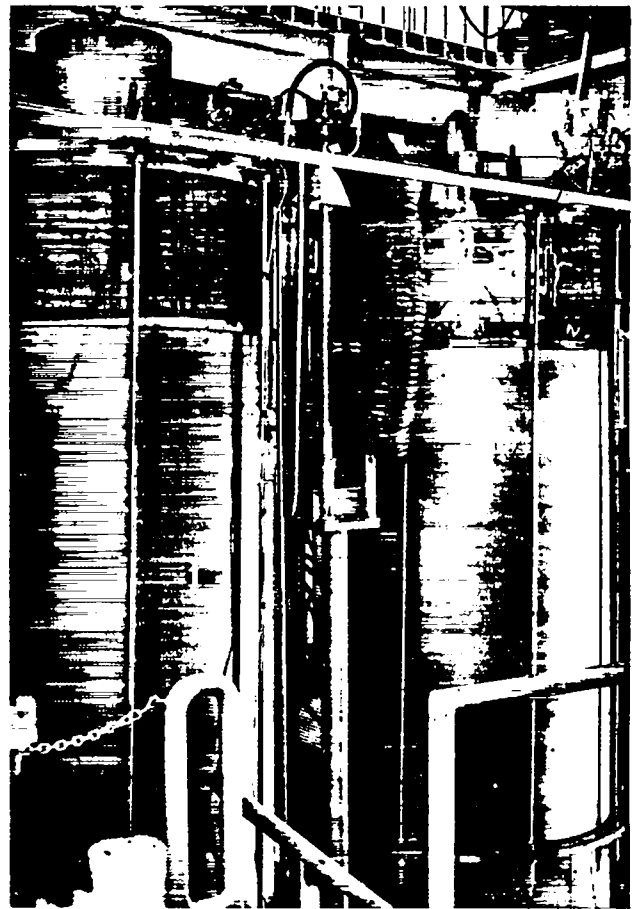


*Fig. 20.*  
*Induction-heated graphitizing furnaces for full-length 19-hole fuel elements.*

**2. KIWI-B4E, Phoebus 1 and 2, and Pewee-1 Coated-Particle Loaded Elements.** The solution to the back-reaction problem was introduction of coated particles. These were 50- to 150- $\mu$ m-diam  $UC_2$  particles coated with  $\sim 25 \mu$ m of pyrolytic graphite. They were introduced with the KIWI-B4E reactors and used from 1964 to 1969 in all LASL and WANL fuel elements.

As noted earlier, the maximum final heat treatment temperature depended on the type of fuel in the element. The first coated particles had a low-density pyrocarbon coat that could not withstand high temperature. At  $\sim 2273$  K (2000°C), the  $UC_2$  core began to migrate through the pyrolytic coating, thus destroying the protection against back-reaction. Consequently, the graphitizing temperatures had to be held to 2173 K (1900°C), somewhat below the point at which the coating was attacked by the uranium core. This temperature



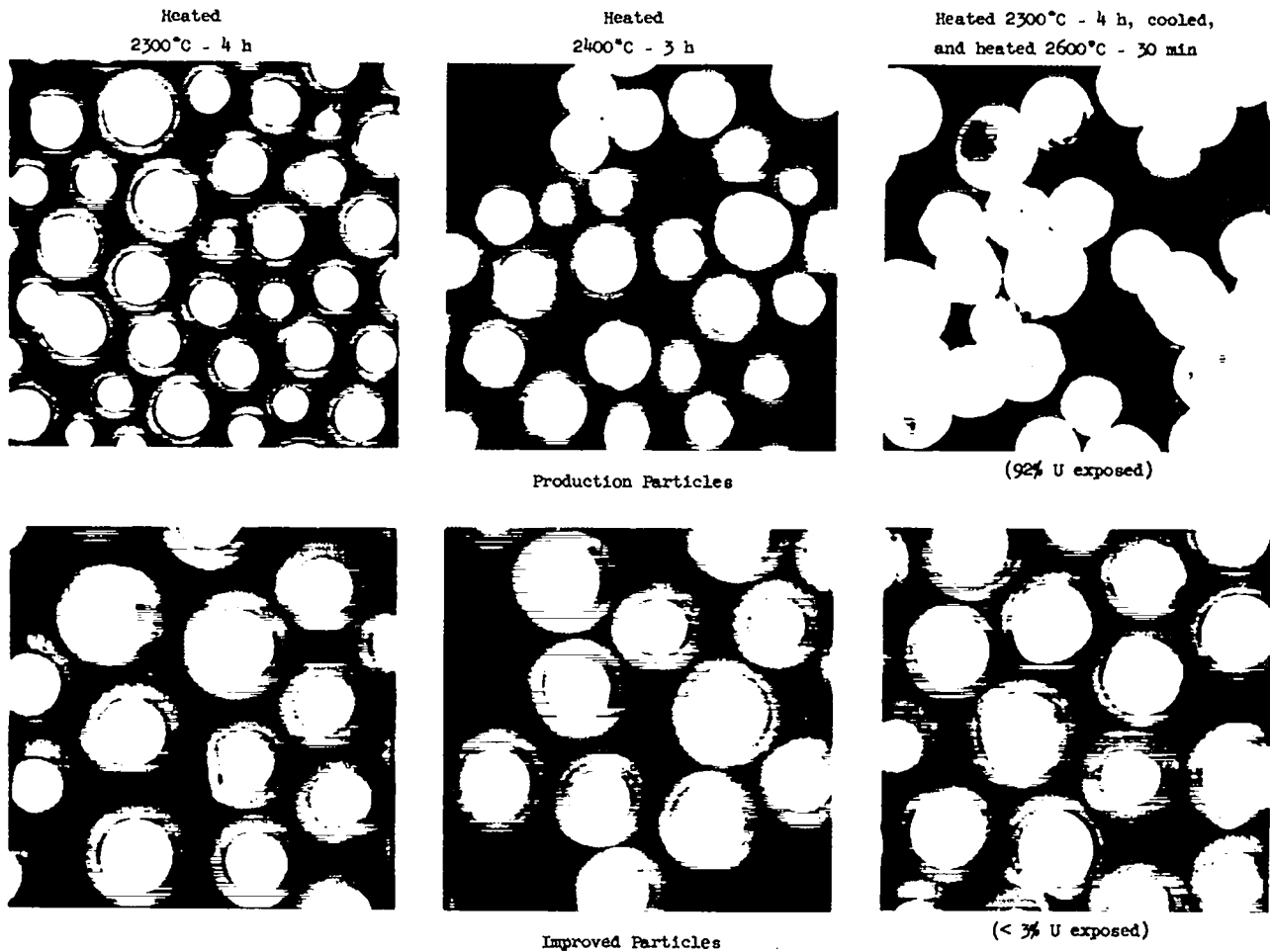


Fig. 22.  
Microradiographs of coated particles.

elements were just part of the information recorded on IBM cards. Elements clad by the niobium tube process were first machined after the boreholes had been machined to the desired diameter, then machined to final length after the niobium tubes had been carbided in their bores. The elements coated by chemical vapor deposition (CVD) were machined to size before coating. All coated elements returned to the shop inspection area for a hole size measurement, using air impedance gauges calibrated to master tubes of known diameter and length.

The machining and inspection of fuel elements were very important development and production steps. The excellent quality of the shop product required innovations and imaginative tool design to cope with the long, small-bore elements. Detailed descriptions of the tooling and procedures are available in the referenced documents.

## VI. FUEL ELEMENT COATING

### A. KIWI-A and -A Prime

The high operating temperature of graphitic Rover and NERVA fuel elements and the required hydrogen propellant made it obvious that the graphite would have to be protected against corrosion if the elements were to survive for a reasonable time. Further, the graphite loss from hydrogen corrosion during reactor operation would seriously affect the reactor system neutronics. Hydrogen and graphite at the anticipated temperatures would react to form methane, acetylene, and other hydrocarbons. Thin, 0.025- to 0.05-mm (0.001 to 0.002-in.) -thick, NbC or ZrC coatings would act as a barrier against hydrogen attack for the length of time the reactor was to operate, so a fuel element

coating effort was undertaken in 1959 for the KIWI-A prime reactor.<sup>19</sup> LASL coating activities involved many people under the direction of M. G. Bowman and T. C. Wallace. John Napier was responsible for fuel element coating at Oak Ridge Y-12, and Charles Hollabaugh supervised similar activities at WANL.

Niobium carbide was selected for the initial work because it has a higher, 3523 K (3250°C), NbC-C eutectic temperature than the 3123 K (2850°C) of ZrC-C. Both NbC and ZrC were expected to resist hydrogen attack at high temperature, and both have relatively low thermal neutron cross sections, although that of Hf-free ZrC would be lower still.

The KIWI-A prime and -A3 fuel elements were relatively short, 216-mm (8.5-in.) -long by 19-mm (0.75-in.) -diam, cylinders containing four axial holes for propellant passage. They were designed to nest into one another to build up the total element length. Seven full-length fuel elements were contained in a length of unloaded, commercial graphite called a module.

Preliminary investigations indicated that NbC could be deposited reproducibly by CVD techniques on the bore surfaces of uranium-loaded graphite tubes. NbC was deposited on the fuel element bores at 1273-2273 K (1000-2000°C) by the reaction of a gaseous mixture of NbCl<sub>5</sub>, HCl, and hydrogen with graphite, using helium gas as a diluent. The reaction



was controlled by the relative reactant concentrations, and the NbC was permitted to form on the graphite surface at a rate controlled by the diffusion of carbon from the fuel element through the NbC layer. A variation of this process, in which methane was introduced into the gas stream, deposited NbC without requiring carbon from the fuel element body to diffuse to the surface. The required fuel element temperature during CVD coating was determined by NDT and sectioning of coated tubes. A compromise had to be reached between optimum coating thickness and acceptable coating taper along the element length. NbC is gradually deposited along the bore length from the gas entrance. The diffusion is controlled by the availability of niobium in the gaseous mixture and by the carbon diffusing to the surface through the deposited NbC layer.

As noted earlier, reaction of bare UC<sub>2</sub> fuel particles with water vapor oxidized the fuel. If the oxide were present during the NbC coating operation, CO evolved at the 2273 K (2000°C) coating temperature would blister the coatings, and it did

early in the coating program. Also, uranium was removed from the bore surface by the HCl reaction with UC<sub>2</sub>. UC<sub>4</sub> (g) is more stable than NbCl<sub>5</sub> or NbCl<sub>4</sub> (g). The following procedure for KIWI-A prime fuel elements was evolved to minimize these problems.

(1) The elements, in batches of 20, were heated to 2373 K (2100°C) in helium to convert the UO<sub>2</sub> to UC<sub>2</sub>.

(2) The temperature was lowered to 1523 K (1250°C), CH<sub>4</sub> was introduced into the system, and the element bore surfaces were coated with a 0.005-mm (0.0002-in.) -thick layer of pyrolytic carbon.

(3) The outside of the element was coated, in a separate operation, with a similar layer of pyrocarbon.

(4) The NbC coating was formed on the bores at 1973 K (1700°C).

The additional equipment available for KIWI-A3, and increased experience in coating fuel elements, allowed us to modify this procedure as follows.

(1) The elements were individually coated with pyrolytic carbon on their exterior surfaces.

(2) The elements were outgassed at 2373 K (2100°C) in a helium stream.

(3) The temperature was lowered to 2023 K (1750°C), and the pyrographite layer was formed on the bore surfaces.

(4) The temperature was raised to 2073-2173 K (1800-1900°C), and the NbC layer was deposited on the bore surfaces.

The higher coating temperature for KIWI-A3 improved the coating adherence and provided thicker NbC coats in the same time. The higher pyrographite bore-coating temperature eliminated trapped gas and reduced blistering.

Development of the proper coating procedure obviously involved development of both coating conditions and coating facilities. Determination of the proper temperature for the NbCl<sub>5</sub> saturator, a powder that vaporized at 483 K (210°C), and selection of the proper mixture of HCl and hydrogen and helium gases to pass through the saturator and deposit NbC coatings of the required thickness were not accomplished easily. Also, the usual problems of cleanliness, surface preparation, equipment modifications, etc. had to be solved to achieve optimum results.

After the KIWI-A prime full-power reactor test, "the general appearance of all fuel elements was excellent." "There were several elements showing blistering and corrosion but not sufficient to damage the modules." Similar observations were made on fuel elements after the KIWI-A3 test. The KIWI-A

prime fuel element coating thickness averaged 0.025 mm (0.001 in.), compared to 0.05 mm (0.002 in.) for the KIWI-A3 elements.

## B. KIWI-B Series

The KIWI-B1A fuel elements were 19-mm (0.75-in.) -diam, ~660-mm (26-in.) -long cylinders containing seven holes for the propellant gas. Two cylinders stacked together made up the fuel element length for the channel in the graphite module. CVD deposition of NbC on fuel element bores had not developed to the point where long, relatively small diameter holes could be coated successfully and reproducibly. Consequently, a different technique was used for KIWI-B1A and several later reactor cores. This technique, very simply stated, was to insert niobium tubes into the fuel element bores and heat the lined elements to the temperature at which the niobium in contact with carbon was converted to NbC.<sup>20</sup>

Thin-walled niobium tubes were obtained from J. Bishop, Malvern, PA or Superior Tube Co., Norristown, PA. The wall thickness specification was  $0.056 \pm 0.013$  mm ( $0.0022 \pm 0.0005$  in.), and the permissible diameter variation was 0.013 mm (0.0005 in.). Twelve tube diameters ranging from 3.86 to 4.42 mm (0.152 to 0.174 in.) were required. Obviously, these specifications challenged the tubing producers, and they probably advanced the art of drawing thin-walled tubing. The cladding procedure also required development work at LASL because the element bores had to be matched with the niobium tubes properly to ensure that the delicate tubes could be inserted into the holes and that the clearances between tube and bore would provide a good, adherent carbide coating. The niobium tube enlarged as it was converted to NbC, and this change had to be considered in dimensioning tubes and boreholes.

All reactors had a large temperature gradient, ranging from a relatively cool 93 K ( $-180^{\circ}\text{C}$ ) where the hydrogen gas entered the fuel elements to the maximum exit gas temperatures. To conserve the expensive niobium tubing, and for neutronic reasons, the fuel element at which the hydrogen gas entered was clad for only about half or less of its bore length because the temperature up to the cladding point was not high enough to cause hydrogen corrosion of the graphite. The downstream fuel element that was subjected to high temperatures was clad throughout its length. The exposed fuel element ends were coated by CVD. This was not a diffusion-

controlled coating as in KIWI-A3, instead the carbide was formed by adding  $\text{CH}_4$  to the coating gases so that NbC, rather than niobium, was deposited on the fuel element.

A very extensive technology for producing NbC-clad boreholes in 7-hole, 660-mm (26-in.) -long to 19-hole, 1321-mm (52-in.) -long elements evolved from this work. The success of the cladding was based on adherence of the NbC to the bore during hydrogen flow at high temperatures. The crack pattern in the NbC coating largely dictated how much protection it provided. As indicated earlier, loss of carbon from the fuel element by hydrogen corrosion would change the reactor neutronics and performance.

The difference in thermal coefficient of expansion between NbC ( $6.6 \mu\text{m}/\text{m}\cdot\text{K}$ ) and the graphite fuel element ( $3.0 \mu\text{m}/\text{m}\cdot\text{K}$ ) cracked the NbC coating during the cooling cycle. Many fine cracks were much less detrimental in the dynamic hydrogen atmosphere than fewer large cracks, and we found that rapid cooling of the carbided element promoted a multitude of fine, circumferential cracks. Therefore, the heat treatment consisted of heating the fuel elements containing the niobium tubes to 2173 K ( $1900^{\circ}\text{C}$ ) in a helium atmosphere, holding at temperature for 2 h to permit the  $\text{UO}_2$  fuel particles to convert to  $\text{UC}_2$ , and then gradually raising the temperature to 2623 K ( $2350^{\circ}\text{C}$ ) and holding for 2 h to convert the niobium to NbC. Then the furnace power was turned off and the fixture containing the carbided fuel elements was pushed into a cooling chamber for rapid cooling in helium. The temperature dropped below 973 K ( $700^{\circ}\text{C}$ ) within 5 min, and the fixture was removed from the chamber within 45 min of the time it was pushed out of the 2623 K ( $2350^{\circ}\text{C}$ ) furnace.

While fuel element coating development and production was under way, another LASL group headed by D. P. MacMillan and L. L. Lyon was setting up an electrically-heated hot-gas test to simulate reactor temperatures and gas flows. Test results were coordinated with NDT results and fed back to the coating development workers to permit modifications in the coating procedures. A set of specifications that each coated fuel element must pass before final acceptance was drawn up.

The above is obviously a very brief, simple description of the complex cladding process developed to produce reactor grade fuel elements. This process was used in making elements for KIWI-B1A through -B4E. Extensive NDT certified each element. Meanwhile, the group working on the hot-gas evaluation test was improving its capabilities. The test for the first clad fuel elements called for a hydrogen flow of 30 kg/h, a maximum fuel element

wall temperature of 2748 K (2475°C), and an exit gas temperature of 2273 K (2000°C) over a 5-min running time at temperature. Test conditions became more severe as coating and testing technology improved. Weight change data and radiography after the test determined the extent of fuel element damage. Representative, acceptable fuel elements showed little or no damage after this hot-gas test.

The KIWI-A prime and -A3 tests in which all fuel elements had exterior pyrolytic graphite coatings to prevent reaction with exposed  $UC_2$  particles showed that the thin coating could retain fission products formed during the reactor run. Thus, radiochemical analysis of such elements after testing provided additional data on the reactor power achieved. Therefore, 42 KIWI-B1A fuel elements clad with NbC also were coated externally with pyrolytic graphite to provide diagnostic information on power levels attained during the reactor run.

### C. Phoebus and Pewee Series

The fuel elements for the Rover and NERVA reactors from Phoebus 1A through the last one were CVD coated.<sup>21,22</sup> This became a very sophisticated

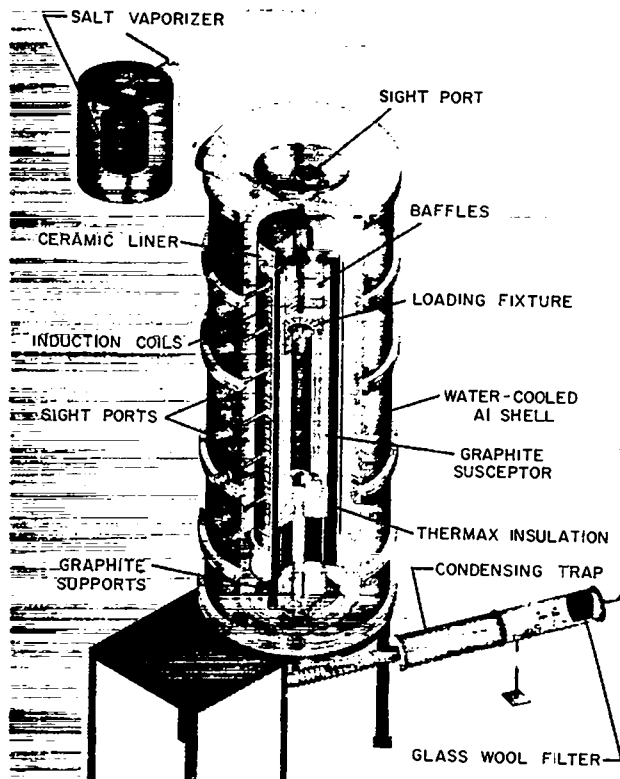


Fig. 23.

Schematic of fuel element CVD coating furnace.

process in which the 19 full-length, 1321-mm (52-in.)-long, 2.36-mm (0.093-in.)-diam bores were coated with NbC or ZrC tailored in thickness over the full length of the element. The early CVD coatings had a useful life of ~10 min, but, by the end of the program, as a result of very extensive development at the three facilities engaged in this work, coatings had been tested successfully for as long as 5 h. Figures 23 through 26 show the coating furnace and the fixtures needed to hold the fuel elements.

The basic coating reaction was the same as that in CVD coating the bores of KIWI-A prime elements. LASL, WANL, and Y-12 evaluated the many parameters that could influence the deposited carbide coat and its adherence to the bore. Coating temperature, gas flow rate, gas concentration, methane in the coating gas, orientation of the element in the coating apparatus, and coefficients of thermal expansion (CTE) of coating and matrix, all influenced the quality of the deposited carbide coat. Details of the coating programs cannot be discussed at length here, so the interested reader should consult the referenced reports. The hot-gas test (described later), in conjunction with extensive NDT and posttest destructive testing, evaluated the quality of the deposited coatings.

One basic problem that plagued the coated fuel elements in the hot-gas and reactor tests was extensive graphite corrosion 381-508 mm (15-20 in.) from the cold end of the element. This so-called midrange or midband corrosion was caused by mismatched

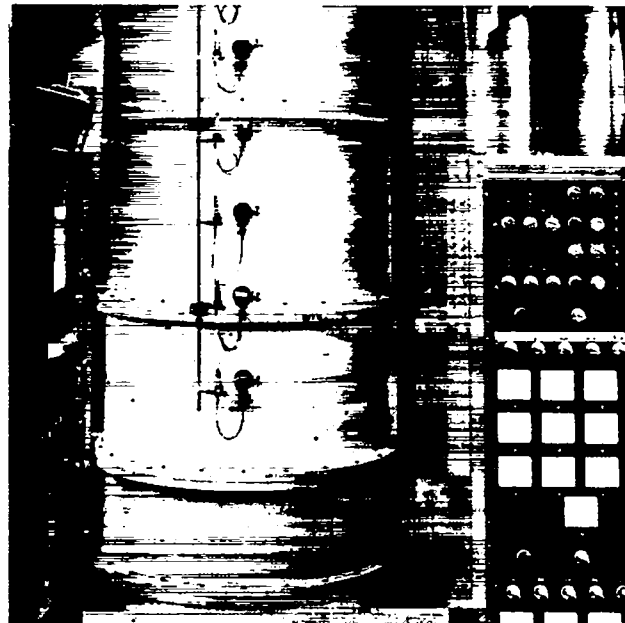


Fig. 24.

Fuel element coating furnace.



Fig. 25.  
Fuel elements in coating fixture.

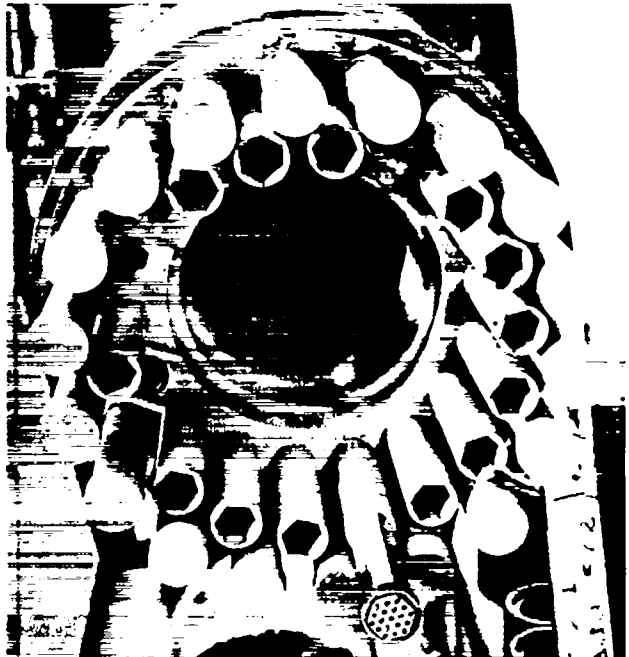


Fig. 26.  
End view of fuel elements in CVD coating fixture.

CTE of the graphite matrix and the carbide coating. On cooling from the coating temperature, the higher CTE carbide coating cracked. The reactor operating temperature in this region was below the coating temperature, so the cracks formed during coating never closed and the graphite matrix was accessible to the hydrogen gas. Many schemes involving wide temperature ranges for coating deposition, overcoating with metal, etc. were tried to solve this problem, but the results were erratic and not very successful or reproducible. The CTE of the fuel elements made of GL 1008 graphite flour was  $3.0 \mu\text{m}/\text{m}\cdot\text{K}$  at 298-1273 K (25-1000°C), whereas that of NbC was  $\sim 6.6 \mu\text{m}/\text{m}\cdot\text{K}$ , over twice as great. The NbC CTE also varied as a function of the C:Nb ratio, ranging from  $6.6 \mu\text{m}/\text{m}\cdot\text{K}$  for a ratio of 0.8 to a high of  $7.35 \mu\text{m}/\text{m}\cdot\text{K}$  for a ratio of 0.97. The high-purity ZrC used on composite fuel elements late in the Rover program had a CTE of  $7.7 \mu\text{m}/\text{m}\cdot\text{K}$  at 293-2273 K (20-2000°C) which increased to  $\sim 9.0 \mu\text{m}/\text{m}\cdot\text{K}$  if the oxygen and chlorine contents were high. The low-purity ZrC also was unstable; upon heating to elevated temperature, the impurity level, as well as the CTE, decreased.

Generally, NbC or ZrC could be deposited in the fuel element bores by either a diffusion or a methane process. Coatings 0.025-0.127 mm (1-5 mils) thick could be deposited at 1473-1673 K (1200-1400°C), contained few impurities, and were stable to above

2273 K (2000°C). When the fuel element matrix CTE matched that of the coating, crack-free coatings could be obtained. The coating CTE varied with the carbon:metal ratio as well as the impurity content.

#### D. Nuclear Furnace-1

The fuel elements in NF-1 were either a new pure carbide (U,Zr)C design or a standard design, 19-hole composite containing uncoated (U,Zr)C particles in graphite. The pure carbide fuel elements were impregnated with zirconium metal by the CVD process late in their processing. The zirconium metal helped fill the pores in the carbide and reacted with the free carbon remaining from the extrusion process to form ZrC.

The composite fuel element bores were CVD coated with ZrC instead of the NbC used on most other fuel elements. Typical CVD coating conditions and the resulting coating thicknesses are indicated in Table II.

At this point, the evaluation process also had become very sophisticated and included high-resolution eddy-current examination to detect cracks, mass per unit length (MULE) determination of deposited coating vs element length, x-ray diffraction analysis to determine lattice parameters, chemical analysis for impurities such as chlorine and oxygen, microstructure determination by optical and scanning-electron microscope, CTE determination, and determination of coating effectiveness in a hot-gas component test that simulated reactor operating conditions.

### VII. NONDESTRUCTIVE TESTING

NDT of Rover and NERVA fuel elements was extremely important.<sup>23</sup> What began as a relatively simple, straightforward quality inspection procedure turned into a sophisticated evaluation (Fig. 27) that was invaluable in development and production of fuel elements.<sup>24</sup> The LASL nondestructive testing was the responsibility of G. H. Tenney and his associates. They undoubtedly advanced the art of NDT by their capable and imaginative efforts to resolve the difficult problems presented to them.

Radiography of the KIWI-A fuel plates, used to determine their soundness, also detected undesirable agglomerates of UO<sub>2</sub> fuel particles. Radiography of the coated 4-, 7-, and 19-hole fuel elements, before and after coating, showed voids, cracks, and inclusions in the graphitized stock and blisters, holes, and thick or thin areas in the NbC-

**TABLE II**  
**CONDITIONS FOR DEPOSITION OF**  
**ZrC COATING IN THE COOLANT CHANNELS**  
**OF A COMPOSITE FUEL ELEMENT**

#### Initial Composition of Coating Gas

Constituents	Flow/Element <sup>a</sup> (m <sup>3</sup> /s, STP)
ZrCl <sub>4</sub>	1.2 x 10 <sup>-6</sup>
CH <sub>4</sub>	0.9
H <sub>2</sub>	66
Ar	66
HCl (first 20 h)	2.6
HCl (last 5 h)	0

#### Deposition Temperature and Coating Thickness

Station from Inlet End (mm)	Deposition Temp (K)	Coating Thickness (μm)
127	1525	60
254	1540	89
508	1580	119
762	1615	132
1012	1640	135
1270	1660	132

<sup>a</sup> Coating time was 25 h at ~ 0.9 atm. This gas flow coated the channel surfaces of one element (0.235 m<sup>2</sup> of surface area).

coated bores. Radiography of slices from various areas of fuel elements showed extrusion patterns that called for modifications of extrusion tooling, as well as the uranium particle distribution throughout the elements.

Fixturing during NDT was important because the orientation of the multihole fuel elements with respect to specific radiographs had to be known. Fuel elements were moved from one area to another in individual aluminum tubes to prevent contamination, and were radiographed in the tubes. The plastic caps for the tubes were designed to fit the fixture so that the tubes could be indexed through 0, 60, and 120° orientation for radiography.

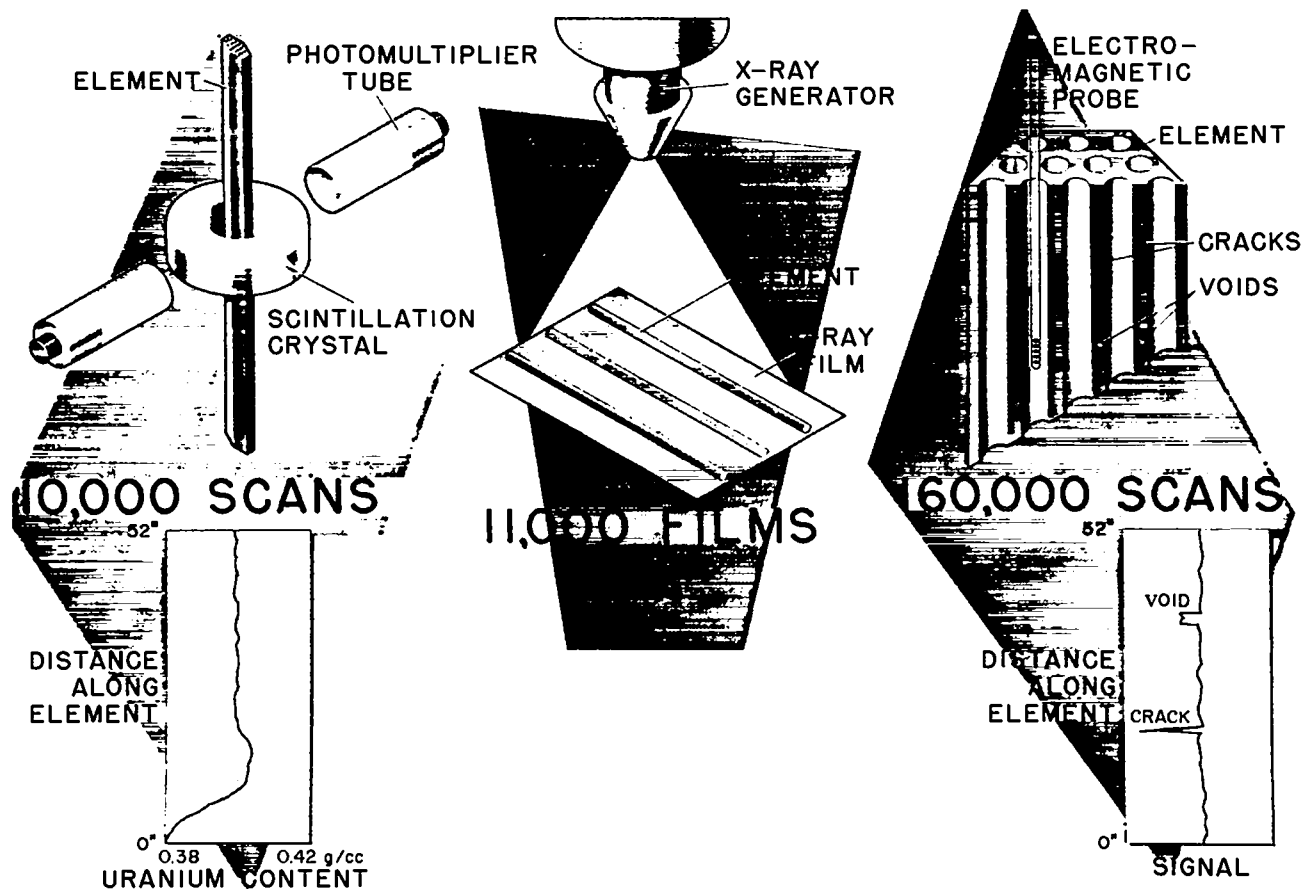


Fig. 27.  
Nondestructive inspection.

The radiographic techniques had to be calibrated as a function of uranium loading to get radiographs of equivalent uranium thicknesses. The elements with high uranium content required significantly higher kilovoltage than those with low uranium content, and the content varied by factors of 2, 3, or more within a given reactor core. The coated fuel elements also required radiographic processing calibration because of the NbC on each bore surface. A set of radiographic specifications for reactor grade fuel elements was developed on the basis of the reactor design requirements and the results of the hot-gas and subsequent reactor tests.

The MULE system, operating on the gamma absorption principle with a  $^{60}\text{Co}$  source, was an extremely valuable development that measured the incremental mass of the fuel element. MULE systems were set up for measurements after coating and hot gas testing and in the NRDS hot cell for reactor-tested fuel elements.

A very important part of the NDT was determination of the uranium content and its distribution

within the fuel elements. Obviously, destructive techniques could not be used during production, and a method for determining the uranium content of each element was essential. The answer was to measure the gamma radiation from the element. The gamma count around an element is proportional to its uranium content. Fuel element standards, calibrated for uranium loading by chemical analysis\* of the samples counted, were used to determine the relationship between observed gamma count rate and actual uranium content. Many gamma-counting instruments were used, including a counter to check the uranium content of the raw extrusion mix against balance weights, a segment scanner for detailed analysis of the uranium distribution along the element length, and a continuous scanner that indicated the average uranium content

\*The LASL Analytical Chemistry Group, under C. F. Metz and G. R. Waterbury, is to be commended for its significant contributions to the Rover program.

of the total element. Along with the actual gamma-counting instrumentation, it was necessary to develop facilities to feed and guide fuel elements through the counters and their automatic recording equipment. Every fuel element produced was counted for uranium content, and its specific position in the reactor core was assigned on the basis of uranium loading. The elements were graduated from high uranium content at the core center to low content at the periphery to give a relatively flat radial fission distribution. In the smaller reactors, there were 10-12 different uranium contents, in the 5000-MW Phoebus 2, ~100 different contents across the core radius.

One very helpful function of the gamma-counting facility was its assistance to the fuel fabricators in determining the uranium mass to load into the green extrusion mix. As noted earlier, uranium content was specified in Megagrams per cubic meter, so density, rather than mass, was really specified. If the fuel element did not shrink properly in processing, its volume would be large and its uranium density low. Conversely, high shrinkage would give high uranium density for the same mass in all cases. A standard cross section, based on the normal dimensional specifications for the element, was established for the gamma-counting calibration. In establishing the amount of uranium to include in the extrusion mix, a so-called loading curve including the calculated uranium mass for each loading step was developed before actual fuel element production. After graphitizing and machining, the elements were gamma counted and then chemically analyzed to compare the uranium mass added to the mix with the actual uranium density. The curve developed from these data determined the mass of uranium added to the extrusion mix at each loading step.

The counting rate correction for gamma absorption by niobium in the NbC coating was determined by using niobium tubes of the proper wall thickness which could be inserted into the bores of 203-mm-long fuel element standards. The ratio of unlined to lined count rate was the correction factor. This factor had to be determined for each type of fuel element, nominal uranium content, and counting system. In production, the average uranium content of a 1321-mm (52-in.) -long fuel element could be determined in 1 min. A 12% random sample from production was checked for uranium distribution using the segment scanner, and these data were obtained from each 1321-mm (52-in.) -long element in 4 min.

Other techniques developed to provide information on coated and uncoated fuel elements included eddy current testing to locate flaws in the uncoated fuel element matrix and cracks in the NbC bore

coating.<sup>25</sup> The beta particle scattering gauge was highly developed and refined to determine the NbC coating thickness along the length of each bore, using a quartz light pipe to couple the scintillator to the photomultiplier. Electron microscopy proved very valuable in describing coating and matrix interaction as well as the coating structure. A number of new NDT techniques were developed as the Rover program continued and as the demand for information about fabricated and NRDS-tested fuel elements increased.<sup>26</sup>

## VIII. NUCLEAR SAFETY

The use of highly enriched uranium (93% U-235) in Rover and NERVA fuel elements required that every proposed fabrication step be evaluated for nuclear safety. At LASL, we were indebted to H. R. Paxton and D. R. Smith, in particular, for their effort in evaluating the operations. Graphite is an excellent thermal neutron moderator, and the enriched uranium was surrounded by graphite both as matrix material and as fixtures during processing. The resin binder was an organic material with appreciable hydrogen content. A processing batch of fuel elements with high uranium loadings could contain as much as 20 kg of enriched uranium. Consequently, enough material was being processed in new and different ways that it would be possible under certain conditions to achieve criticality.

The size of the batch in the P-K blender and the amount of enriched uranium that could be loaded into the thick steel extrusion cylinder were limited as a result of mockup experiments by nuclear safety personnel. The number of elements in fixtures in the curing oven was limited, and groups of fixtures had to be separated by an air gap, Fig. 28. One restriction concerned dispersion of fuel elements during baking and graphitizing when the respective fixtures each held 90 fuel elements containing many kilograms of enriched uranium. The baking furnace

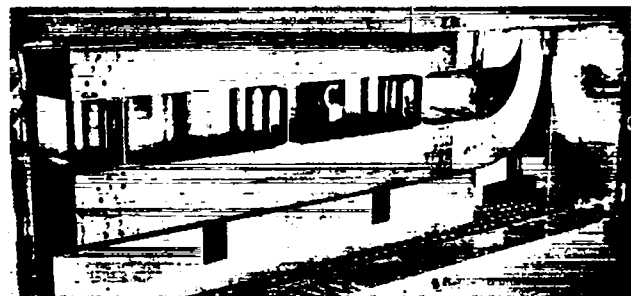


Fig. 28.

*Fuel elements in curing oven showing separation of fixtures.*

was a completely dry system with no water cooling available inside it. The prescribed baking fixture was a solid graphite cylinder containing holes for 90 elements. The graphitizing furnace, on the other hand, was inductively heated and the induction coils were water-cooled. An undetected water leak inside the closed furnace could flood it completely. The fuel element fixture was annular in cross section but contained the same 90 fuel elements. This distribution of uranium would not go critical in a flood, whereas the solid fixture with the same number of highly loaded elements could go critical. Fig. 29 shows both types of fixtures.

During fuel element CVD coating, a certain amount of uranium leaching occurred as the coating gas passed over the fuel particles exposed on the bore surfaces. A safe-geometry trap was developed which would collect the uranium and be safe even in a flood.

Any proposed modification to equipment or processing details always was submitted for nuclear safety review before any action was taken. Such reviews are a necessary part of work with fissile materials.

## IX. FUEL ELEMENT AND TIP JOINING

The 19-hole hexagonal fuel elements introduced with the KIWI-B4 reactor were bore-coated with NbC by the CVD process. The hot end of the element which rested on the composite refractory carbide-graphite support block also was CVD coated with NbC. Early coating evaluations showed that NbC did not adhere to uranium-loaded graphite so well as to pure graphite. In particular, the coating at

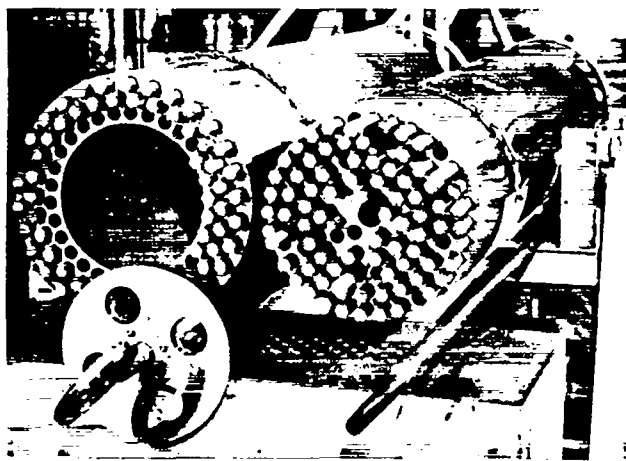


Fig. 29.

*Graphitizing (left) and baking fixtures for 90 fuel elements.*

the hot end of the element tended to flake, exposing it to hot hydrogen gas and causing corrosion. Also, the NbC coating adhered very strongly to the composite carbide and graphite support block, a material containing 40 wt% NbC-40 wt% TaC-20 wt% C (46 vol% carbide-C) prepared by hot pressing. In fact, it was impossible to remove the NbC coating from this material except by grinding. It was proposed that a short tip of the composite be bonded to the end of the fuel element to eliminate the serious corrosion at the fuel element and support block interface.

### A. Gluing

Tip stock of the same composition as the support block was prepared by hot pressing and then machined into a hexagon with the same 19-hole configuration as the fuel element. Techniques were developed for bonding the long composite tip to the end of the element with a graphite cement, P-514,\* before the element went through final machining. LASL also successfully used a mixture of Varcum resin with 40 wt% fine graphite powder as a graphite cement. The machined end of the fuel element had to be leached in HCl to remove the exposed UC<sub>2</sub> particles. After the tip had been applied with the graphite glue and held in place with wire fixtures, the joint was heated to polymerize the resin in the glue. The glued tips were well bonded to the elements and could proceed through final machining of the 19 holes and the hexagonal outside contour without separation. However, several lengthy processing steps were necessary.

WANL made an extensive investigation of the possibility of bonding adjacent fuel elements with the carbonaceous cement.<sup>27</sup> The Rover and NERVA reactor cores were composed of 19-hole hexagonal elements that had to be assembled into the core one at a time. The WANL experiments were aimed at producing clusters of 7 or 19 fuel elements and support pieces. The investigation was terminated, but the strength, thermal shock, and other results obtained on cemented clusters were very encouraging.

### B. Brazing

A tip-brazing procedure was developed which reduced the processing time and produced a very strong bond between tip and fuel element. Carbide-forming elements in Groups IV A (zirconium), V A (tantalum), and VI A (molybdenum and tungsten)

\*Manufactured by Great Lakes Carbon Company.

were evaluated along with the temperature and time relationship for production of good bonds. A fully diffused joint, in which the brazing material was heated to its carbide-carbon eutectic temperature and the joint interface essentially disappeared, produced the strongest bonds and was not temperature-limited in use.<sup>28</sup> An interface in which the bond contained a carbide layer such as TaC, because its carbide-carbon eutectic temperature was too high, produced a much weaker, more brittle bond. Molybdenum and tungsten both have carbide-carbon eutectics at reasonable temperatures and gave fully diffused joints and strong bonds. Bond strengths were evaluated in room-temperature fixture tests and high-temperature tensile tests, and the fully diffused joints were as strong as the parent graphite.

Foils, as well as powders, of the brazing material could be used successfully. Molybdenum, tungsten, and zirconium foils 0.013 mm (0.0005 in.) thick were blanked to produce a 19-hole, hexagonal configuration. Powders could be spread on one surface by wetting it first with a small amount of resin to which they would adhere. The tip and fuel element joint was heated locally by an induction coil powered by a 450-kHz power unit. Brazing thus replaced cementing in fuel element production. Figure 30 shows the tip-brazing facility.

Development of the composite fuel element sometimes called for brazing tips onto elements or brazing together different types of elements. Consequently, in development work, we brazed fuel elements to tips, to other fuel elements having

different volume per cent uranium loadings, and to bead-loaded elements. The tips were machined from hot-pressed NbC-TaC-C composite containing 46 vol% carbide. When brazing tips to fuel elements, we used a transition piece of 30 vol% ZrC-C composite material between tip and element. We brazed the tip to the transition piece and brazed this assembly to the element, in two separate operations. The transition piece was necessary because of the Mo-UC<sub>2</sub> low-temperature eutectic that would produce a liquid component at the 2923 K (2650°C) molybdenum brazing temperature. Therefore, we brazed the refractory carbide composite tip material to the 30 vol% ZrC transition piece using molybdenum at 2923 K (2650°C), and then brazed this assembly to the fuel element at 2623 K (2350°C) using (U,Zr)O<sub>2</sub> powder.

## X. FUEL ELEMENT EVALUATION

### A. Hot-Gas Testing

Different types of enriched uranium fuel, extrusions, heat treatments, and coating parameters were being investigated while fuel elements for specific reactor cores were in production. It was obvious very early that a test that simulated reactor operating conditions, without radiation, would be extremely valuable in evaluating progress in the various development programs. The test would require electrical heating to achieve the desired temperature, and it should provide the same

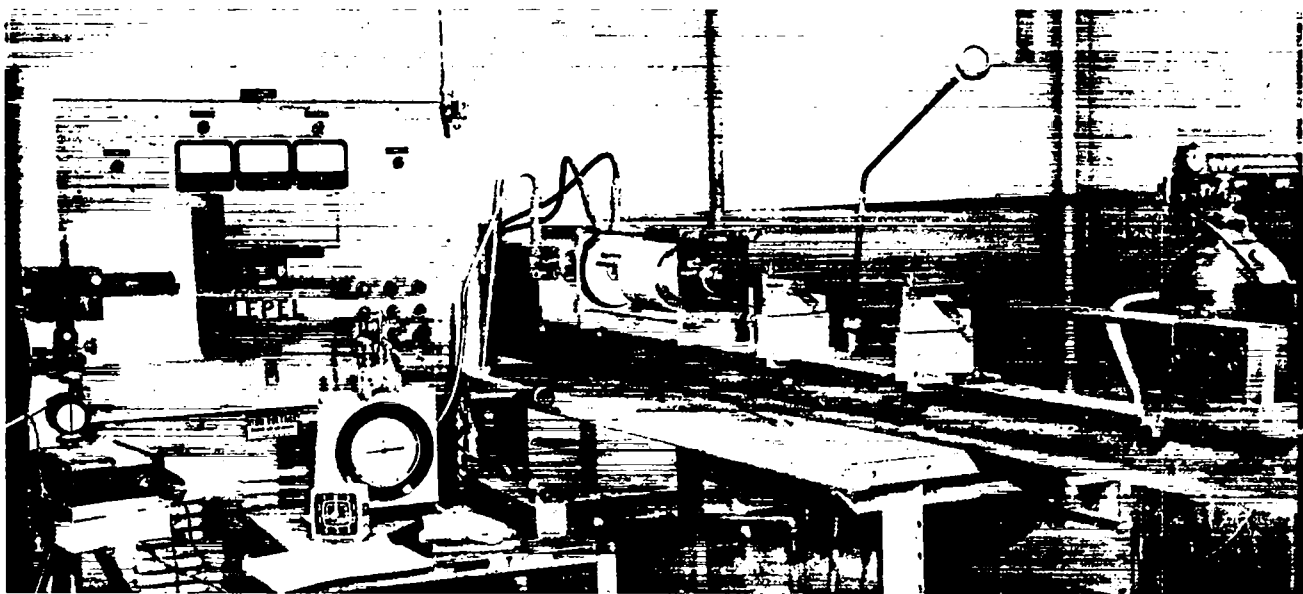


Fig. 30.  
The tip-brazing facility.

temperature gradients that a fuel element encountered in a reactor core. It should also provide hydrogen gas at reactor pressure and flow conditions to flow through the heated fuel element. In a very significant achievement, LASL developed a fuel element test facility under the direction of D. P. MacMillan and L. L. Lyon. A similar facility was installed at WANL, under Morton Blinn.

We built a high-pressure furnace in which the fuel element under test was the resistive heater element. The hydrogen gas passed through a preheater before entering the fuel element bores (Fig. 31). This type of furnace required a substantial amount of electrical power as ~1 MW was required to heat each fuel element. The original power supply was a 10-MW bank of US Navy submarine batteries that had been retired from regular service. Later, motor generator rectifier power systems replaced the batteries.

The furnace (Fig. 32) was installed in a reinforced concrete cell, and the operators read fuel element temperatures by focusing telescopes through windows in the cell and sighting ports built into the furnace. Obviously, successful operation of such a furnace required much engineering and materials

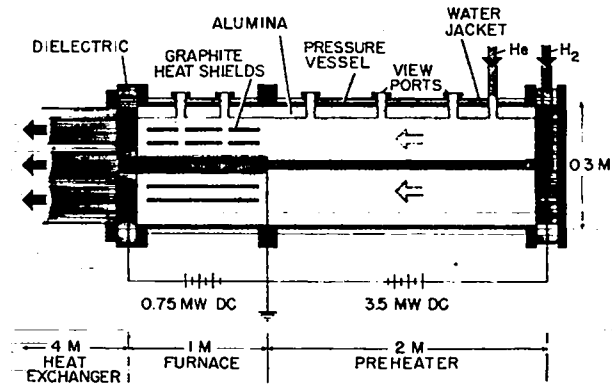


Fig. 31.  
Schematic drawing of hot-gas test furnace for Rover fuel elements.

development to cope with the extreme temperatures, high current, and hydrogen environment.

The furnace tests provided a reasonable simulation of reactor power density, temperature, and thermal stress and of the effects of flowing hydrogen.

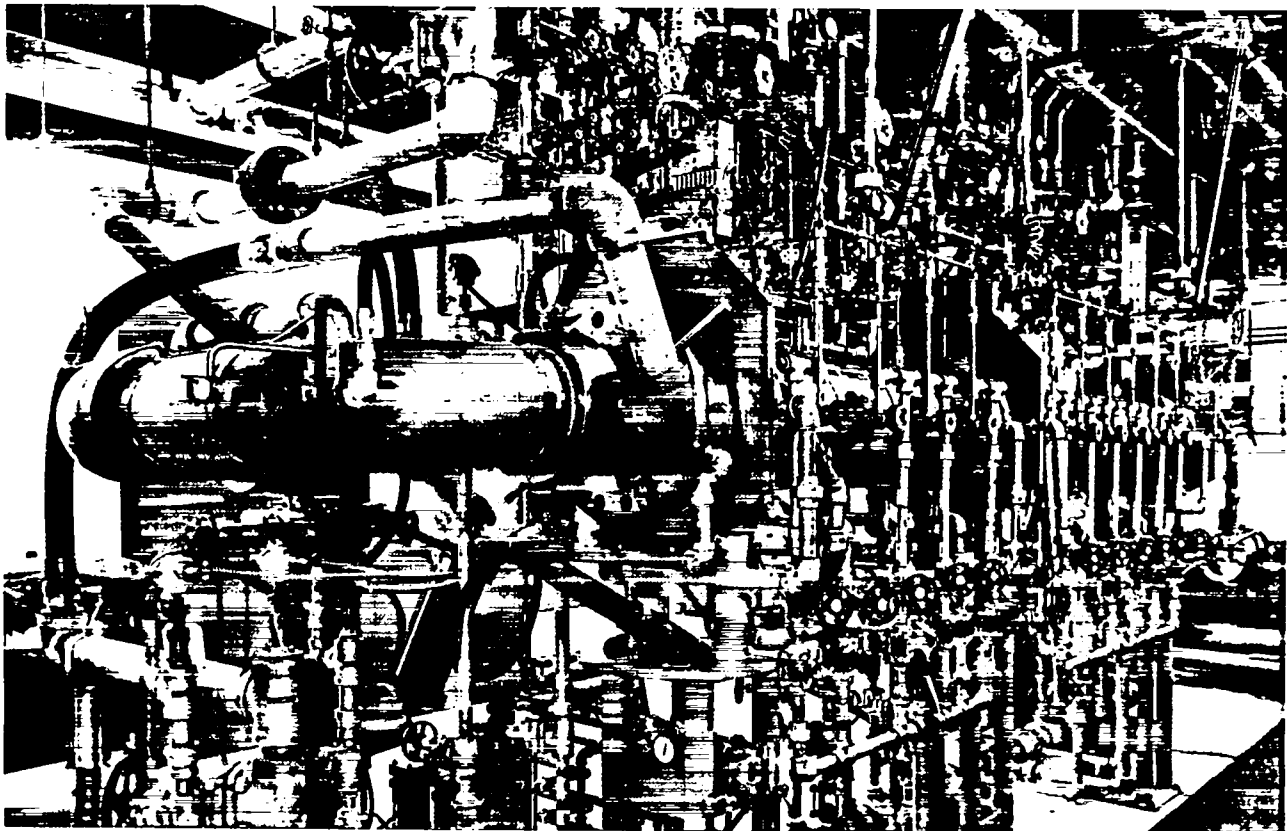


Fig. 32.  
The hot-gas test furnace.

Of course, they gave no information about radiation damage, but it was felt that the very high temperature and very small burnup in reactor operations would minimize the radiation effect. There was some concern that the volume heat generation produced by ohmic heating was a poor simulation of nuclear heating. Changes in fuel element composition which affected the electrical conductivity of the element created problems. In general, however, furnace testing was very valuable in development of new fuel element technologies and also in quality control sampling during manufacture of fuel elements for specific reactor cores. Unfortunately, no report describing the total hot-gas testing program was ever prepared. Further information can be obtained only from LASL Group N-1 progress reports.

The fuel elements were extensively NDT evaluated before and after hot-gas testing, to determine what changes occurred. NDT determined the midrange corrosion very accurately. Tested fuel elements also were sectioned along their entire length to expose the five central holes and show the condition of the coating and matrix after the hot gas test. This sectioning provided information about the protective capability of the carbide coating.

## B. Thermal Stress Testing

Thermal stress testing of Rover and NERVA fuel elements also required extensive new procedures. The fission energy generated as heat in the fuel was conducted through the graphite matrix and NbC coating and removed through convection by the hydrogen propellant. The heat conducted to the coolant channels created temperature gradients across the element which induced thermal stresses in the matrix. Because cracks or fractures would expose the matrix to corrosion by hot hydrogen, fuel elements had to retain structural integrity throughout reactor operations. The extremely fast startup of the nuclear rocket engine and the possibility of reactor scram with rapid cool-down also created worry about thermal stress and the behavior of fuel elements in such situations.<sup>29</sup>

A test program was developed at LASL under the direction of J. C. Rowley, and SNPO awarded a contract to F. J. Witt at ORNL for thermal shock testing of Rover and NERVA fuels. Two types of tests evolved. The ZAP test evaluated thin wafers cut from the ends and middle of elements. This test of graphite fuel element thermal shock characteristics was developed at ORNL and adapted for use at LASL.<sup>30,31</sup> The ZAP test, very simply, shocked the thin specimen by arcing it with a

welding electrode powered by a welder power source, thus introducing a high current into it. The minimum wattage required to fracture the test wafer was taken as a measure of its thermal shock resistance.

The objective of the LASL thermal stress program was to determine the power generation and thermal stress limitations of fuel elements over a range of temperatures. The thermal stress test evaluated 368-mm (14.5-in.) -long test samples machined from full-length elements.<sup>32</sup>

A sizeable calculational effort accompanied the experiments to establish the power density and thermal stress limitations of the 19-hole hexagonal fuel elements. Computer codes were developed to predict fuel element behavior and to correlate the experimental results.

The experiments involved development of apparatus in which the 368-mm (14.5-in.) -long sample was heated electrically by a 20-MW storage battery. The current passed through the sample ranged from 5000 to 10 000 A to produce wall temperatures as high as 3073 K (2800°C). Hydrogen flow rates varied, but were several hundred kilograms per hour. The normal procedure was to subject each specimen to progressive thermal loading until it fractured.

The temperature was controlled by varying the hydrogen flow rate through the specimen. The working length of the specimen was the central 178 mm (7-1/4 in.), and specimen power generation was determined to a precision of  $\pm 1\%$ , from the current flow and voltage drop across this length. The experimental data were logged simultaneously on analog records and by a digital data acquisition system.

Many variations were used to produce or delay fracture in thermal stress evaluation. Holes were plugged, radiation shields were used, holes were misplaced from true position, etc. to produce thermal gradients in the fuel element section. In the NbC-coated samples, some of the current was carried in the bore coatings and the amount varied with coating thickness. For example, at an outer surface temperature of 2273 K (2000°C), a 0.025-mm (1-mil) -thick NbC coat generated about 8% of the total power and a 0.05-mm (2-mil) coat generated approximately twice as much. Typical thermal stress failures started with formation of a longitudinal crack usually followed by a transverse break. The thermal stress test results were reported in terms of power density ( $\text{MW}/\text{m}^3$ ) in the specimen, and the test became an important tool for evaluating new fuel element materials. Figure 33 shows how carbide content influences the thermal stress resistance of composite fuel elements.

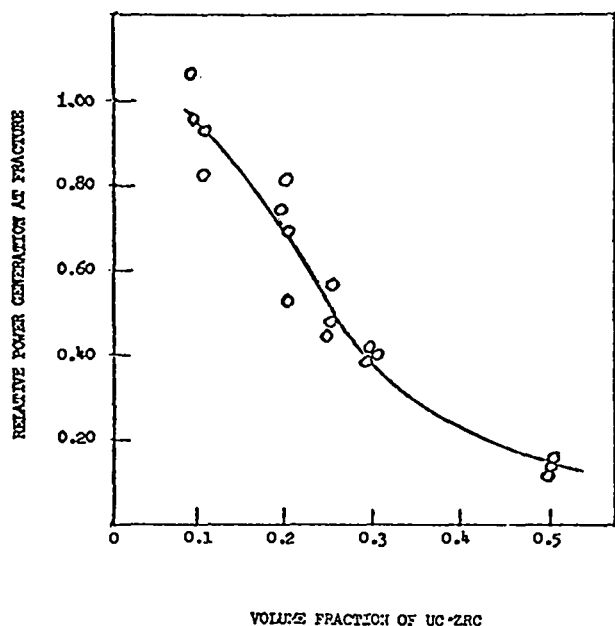


Fig. 33.

Effect of carbide content on composite fuel element thermal stress resistance.

## XI. ADVANCED FUEL ELEMENTS

The KIWI, Phoebus, and Pewee fuel elements had a graphite matrix protected against hydrogen corrosion by a NbC coating. As fuel element technology improved, it became possible to operate reactors at maximum matrix temperatures of 2373-2573 K (2100-2300°C) for as long as 1 h. Carbon loss from the elements after 1 h of testing was great enough to affect the reactor core neutronics adversely. Development of new fuel elements that would be highly resistant to hydrogen attack and could be used at high operating temperatures was undertaken. Three approaches were considered.

- (1) Changing the graphite flour and binder to new materials whose CTE values matched that of the coating and using only graphitizable constituents.
- (2) Retaining the 19-hole hexagonal design, but using a composite carbide and graphite matrix.
- (3) Designing a new, all-carbide, fuel element.

Much effort went into fabrication and evaluation of high-CTE graphite and composite carbide and graphite elements, and a lesser effort was devoted to the pure carbide. However, enough progress was made so that the last reactor test at NRDS, Nuclear Furnace-1, was fueled with both composite and carbide elements.<sup>33</sup> NF-2 was to include high-CTE graphite fuel elements, but the program was cancelled before the reactor could be run.

### A. High-CTE Graphite Elements

The serious midrange corrosion of uranium-loaded graphite fuel elements was attributed directly to the large CTE difference between the graphite matrix ( $\sim 3 \mu\text{m/m}\cdot\text{K}$ ) and the NbC ( $6.6 \mu\text{m/m}\cdot\text{K}$ ) or ZrC ( $7.7 \mu\text{m/m}\cdot\text{K}$ ) coatings applied to the 19-hole element bore surfaces. The Oak Ridge Y-12 plant worked hard to obtain or develop graphite or filler flours with high CTEs and binders that would graphitize during the high-temperature fuel element treatment.<sup>34</sup> Another practical reason for the investigation was the nonreproducibility of the commercial flours and binders. A synthetic material, produced under carefully controlled conditions, could be the answer to long-range, high-volume production of reactor grade fuel elements.

The Y-12 plant evaluated commercial materials and made an in-depth study of organic carbon precursors, binders, fillers, and manufacturing processes related to the new materials. They evaluated small quantities of 11 different commercial graphite flours whose CTEs were greater than that of the standard type 1008 flour. Table III lists the flours and their CTEs.

The fuel elements produced did have higher CTEs than elements made with the standard flour, and cracking in the NbC coating decreased as the matrix CTE increased. Also, the thermal stress resistance of the element tended to decrease with increasing CTE.

Phase II of this study involved larger quantities of eight commercial graphite flours selected from Phase I. The binders were the standard Varcum and a graphitizable resin of isotruxene (ITX), acenaphthalene (ACN) polymer, and indene developed at Y-12. The resulting fuel elements had CTEs as high as  $6.5 \mu\text{m/m}\cdot\text{K}$  at 298-2273 K (25-2000°C). Also, the thermal stress resistance of high-CTE elements was improved if the graphite matrix had a high flexural strength, low modulus, and high strain-to-failure value.

The attempt to develop a graphitizable binder to replace the "glassy" carbon of the Varcum resin yielded four different binders. All were modified with indene, permitting extrusion at room temperature, and all produced a graphite phase after high-temperature heat treatment. The four binders were ITX-ACN-I, cinnamylideneindene-indene (CAI), Grade 277-15V\* pitch indene, and Grade 240\*\* pitch indene. The indene addition changed the extrusion mix viscosity successfully; a nominal 250 cP was the target value for room-temperature extrusion capability.

\*A product of Allied Chemical Company.

\*\*A product of Ashland Oil and Refinery Company.

TABLE III  
COEFFICIENTS OF THERMAL EXPANSION

Flour Type	CTE (298-2273 K, $\mu\text{m}/\text{m}\cdot\text{K}$ )
GL 1008	3.31
ZTA	3.67
Graph-i-tite "G"	3.92
Stackpole 2033	4.56
Gilsonite	4.56
Speer SX5	5.21
POCO AXZ90	5.28
POCO AXZ	5.41
POCO AXM90	5.47
POCO AXF90	5.70
POCO AXM	6.51

The attempt to develop a reproducible synthetic filler flour to replace the commercial graphite flour introduced another concept that would improve fuel element properties and behavior. The commercial graphite flours had been taken to high temperatures and were dense, stable particles. It was postulated that a matrix with minimal internal stresses could be made if the filler particles would shrink while the binder was shrinking, preferably both at the same rate. Consequently, the development phase included matrix filler particles that were only low-fired, not thermally stabilized. The resulting fuel elements, prepared with different flours and binders, yielded interesting but widely differing results. Details of the experimental work and evaluation data are given in Ref. 34.

As a result of the above program, Y-12 prepared a number of fuel elements for the NF-2 reactor test which, unfortunately, was cancelled when the Rover and NERVA program was halted. The fuel elements were made with low-fired, 1173 K (900°C), POCO PCD(-9) Q carbon filler and Ashland 240 pitch-indene binder. These elements, coated with ZrC, had an average CTE of 6.5  $\mu\text{m}/\text{m}\cdot\text{K}$  at 298-1273 K (25-1000°C), not far from the ZrC value of 6.9  $\mu\text{m}/\text{m}\cdot\text{K}$ . The fueled elements (385 Mg U/m<sup>3</sup> of coated particles) had an average flexural strength of 53.7 MPa (7785 psi), whereas unfueled elements averaged 81.6 MPa (11 830 psi). The NF-2 element strain to failure was 4150  $\mu\text{in.}/\text{in.}$  compared to the standard element value of 3000  $\mu\text{in.}/\text{in.}$  The NF-2 thermal shock and thermal stress resistance also were higher than those of previous elements made from the standard flour and Varcum binder.

The program was halted before any of the materials or manufacturing processes could be optimized. The very promising results, however, indicate that these materials should be seriously considered in any future graphite fuel element work.

## B. Composite Elements

Interest in a composite fuel element was generated by the excellent high-temperature performance of the refractory carbide-carbon composite tips and support components. This material has a high-temperature capability and an extremely adherent NbC coating and, in case of coating failure, loses carbon only immediately around the uncoated area and retains its integrity as a support member. It contains 46 vol% NbC-TaC in carbon and has a carbide matrix.

Because of these properties and the LASL and Y-12 experience in extruding refractory carbide composite tip stock, we selected a UC-ZrC-C composition to yield ~50 vol% total carbide with an ~500-Mg/m<sup>3</sup> uranium loading and an ~3.4- $\mu\text{m}$  carbide particle like that of the NbC and TaC in the structural composite. The graphite flour used in most of the composite development was our standard S97 grade, and the binder was Varcum resin. Thermax also was used in the mix.

There are several ways to arrive at the solid solution of UC-ZrC. It can be made as UC-ZrC powder which is then used as the starting material, or it can be made *in situ*; that is, by forming the solid solution during the thermal treatment of the composite fuel element. We had had extensive experience with UC-ZrC powder, although of a higher uranium content, and it tended to oxidize. The relatively low uranium content of the Rover UC-ZrC made this less of a problem. It would also be necessary to make UC-ZrC powders with many different uranium contents to satisfy reactor loading specifications. For these and other reasons, we decided to investigate other techniques for making the solid solution.

UO<sub>2</sub> had been well characterized at LASL, and it was used as the uranium source in the solid solution carbide. Zirconium compounds for the fuel elements had to be reactor grade (low Hf), and both ZrO<sub>2</sub> and ZrC were investigated. The ZrO<sub>2</sub> starting material was eliminated because the carbon loss from the ZrO<sub>2</sub> + C reaction was serious enough to degrade the mechanical properties of the fuel element.

When we changed the materials or compositions for fuel element extrusions significantly, we normally did not make 19-hole extrusions immediately. We used a small extrusion press with small charges and

extruded a 6.35-mm (1/4-in.) -diam tube containing a 2.54-mm (0.1-in.) -diam hole to determine the proper binder level and discover any extrusion problems. These tubes went through all the subsequent thermal cycles as part of their overall evaluation. Thus we did much development work on small tubes before extruding any 19-hole fuel elements.

The process evolved for making composite fuel elements was very like that for the coated-particle elements.<sup>35</sup> The extrusion mix contained reactor-grade (low-Hf) ZrC, UO<sub>2</sub>, and the regular flours and binder used in all previous elements. The same low-temperature, through 1123 K (850°C), heat treatments noted earlier were used for the composite elements. The high-temperature (graphitizing) treatment was performed in two steps, primarily to control fuel element distortion by changing the holding fixtures. The first high-temperature treatment was to 2623 K (2350°C) with the temperature held for two or more hours. X-ray diffraction of the fuels after this treatment always showed single-phase, solid-solution UC-ZrC. The final heat treatment depended on the uranium content of the carbide and the total volume per cent of UC-ZrC, but temperatures were ~2973 K (2700°C).

We did encounter several fabrication problems in changing to the carbide fuel. The carbides are very hard and abrasive, and we did not want to have to ream or grind the nineteen 1321-mm (52-in.) -long, small-diameter holes in each element to the required size. Consequently, we undertook to extrude the holes to size to eliminate this operation. We were able to control the shrinkage well enough after the final heat treatment at 2973 K (2700°C) so that we could design the pin size and location in the extrusion tools to produce holes in the final graphitized element within  $\pm 0.038$  mm (0.0015 in.) of desired diameter and in the proper location. Thus, the fuel elements required grinding only on the exterior hexagonal surface for finishing, a very significant time and cost savings.

Another problem was the weight of the carbide-loaded element and the increased friction as the green extrusion moved from the extrusion die along the graphite fixture. The friction was so great that the last section of extrusion tended to compress and bulge rather than slide. After heat treatment, the elements tapered seriously from end to end. They were oversize at the rear and tapered to normal size at the front. After much experimentation, we evolved the air-vein fixture (Fig. 34), in which low-pressure air was introduced through a series of small holes under the extrusion. The heavy fuel element thus moved on a film of air, the sliding contact and frictional pull were minimized, and the taper in the element was eliminated.

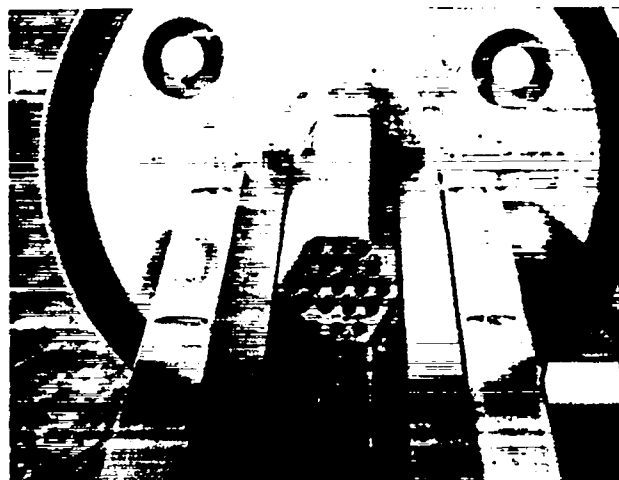


Fig. 34.  
*Composite fuel element being extruded into air-vein fixture.*

The hardness and abrasiveness of the carbide fuel loading also became evident during extrusion. There was very severe wearing, particularly of the hardened steel die pins that determined the size and location of the 19 holes in the element. This was especially important, as we were extruding the holes to a size that would shrink to the proper diameter during final heat treatment. Therefore we started evaluating wear-resistant materials for die components. We eventually selected Ferro-TiC Grade C\* from about a dozen materials evaluated, and it worked extremely well with abrasive materials. Ferro-TiC Grade C has a Rockwell C hardness of 70 and contains a high volume of TiC particles in a steel matrix. It is not so ductile as regular steel, and pin breakage in the extrusion tooling increased, but we could live with that problem if we obtained the other desired advantages.

The total volume per cent of carbide (UC + ZrC) loading was dictated by the properties of the resulting fuel elements. If the carbide loading were too low, the element would have a graphite matrix, not a continuous carbide network, and would lose integrity if the free carbon was corroded away. If the carbide content were too high, the element would have undesirable thermal stress characteristics. The first experiments produced a 50 vol% carbide composite fuel element, but the thermal stress tests were disastrous.

A parallel program had been undertaken simultaneously to evaluate how carbide content

\*A product of Sintercast, West Nyack, NY.

affected extruded composites. We made 19-hole extrusions whose carbide content was varied from 10-40 vol% in 10% increments. NbC was used as the carbide. Samples were tested for thermal stress, and the results were very encouraging. Thermal stress resistance was high at 10 vol% NbC and decreased as the carbide content increased to 40 vol%. Moreover, at 20 and 30 vol% carbide, the thermal stress resistance was considered adequate for reactor conditions.

We then tried lower total carbide loadings and prepared (U,Zr)C-C composite fuel elements with 20, 25, 30, and 35 vol% total carbide. The thermal stress resistance improved dramatically at the lower levels, and after experimentation we settled on 30-35 vol% total carbide content. This composition had both continuous carbide and graphite structures. Although the uranium content had to vary as a function of element location in the reactor core, the total UC and ZrC carbide content was held constant. Again, the final high-temperature heat treatment of the composite fuel elements was the critical parameter that determined how well they performed in the evaluation tests.

The phase equilibria in the carbon-rich part of the U-Zr-C ternary system are shown in Fig. 35 as a vertical section passing through the ZrC-C and UC<sub>2</sub>-C eutectic points. Figures 36 and 37 show portions of the "pseudo-binary" phase diagrams of interest for 30 and 35 vol% carbide composite fuel elements. The solidus, eutectic, and solvus lines intersect at

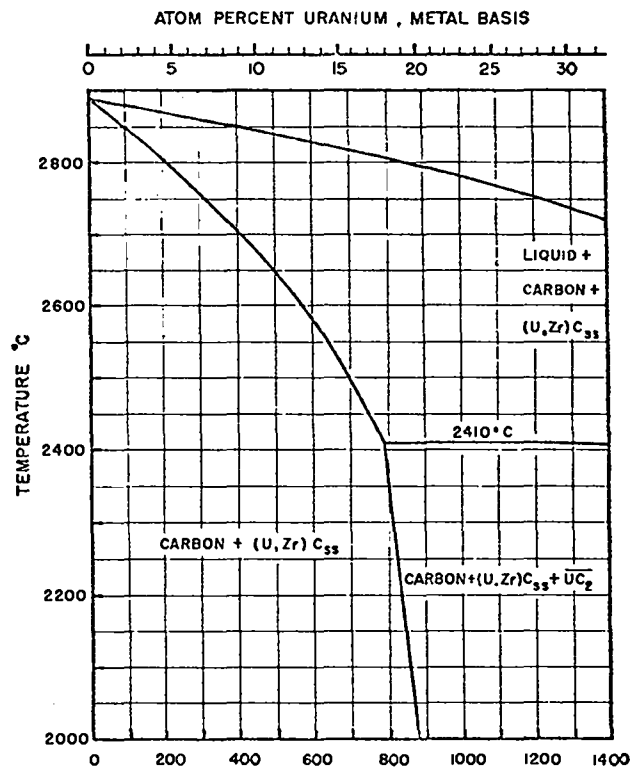


Fig. 36.  
Phase diagram for 30 vol% carbide.

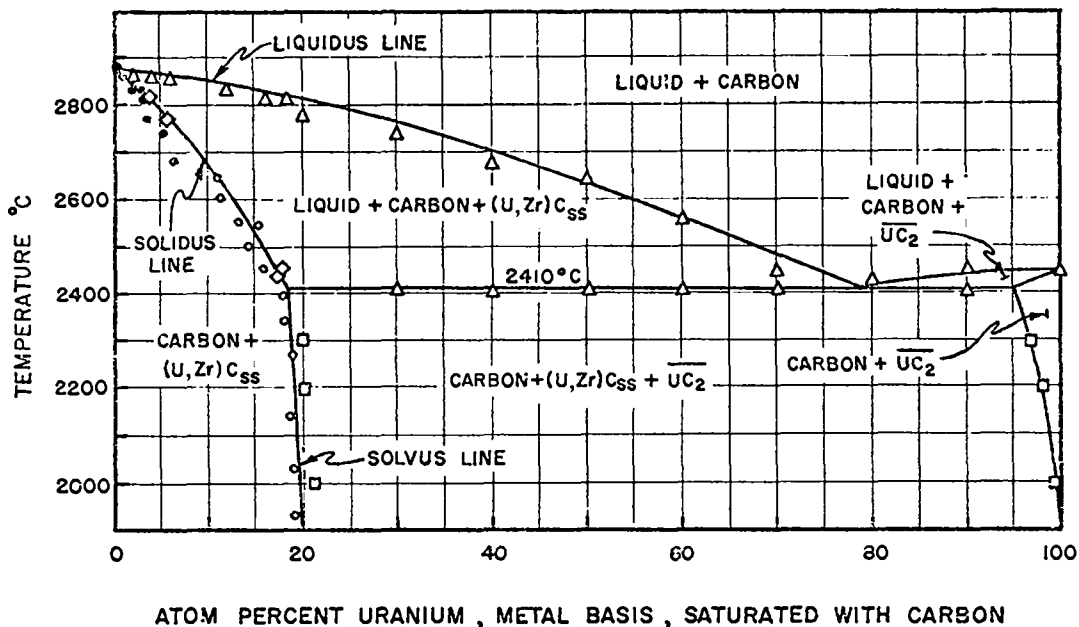


Fig. 35.  
Phase equilibria in the high-carbon portion of the U-Zr-C ternary system as a vertical section passing through the ZrC-C and UC<sub>2</sub>-C eutectic points.

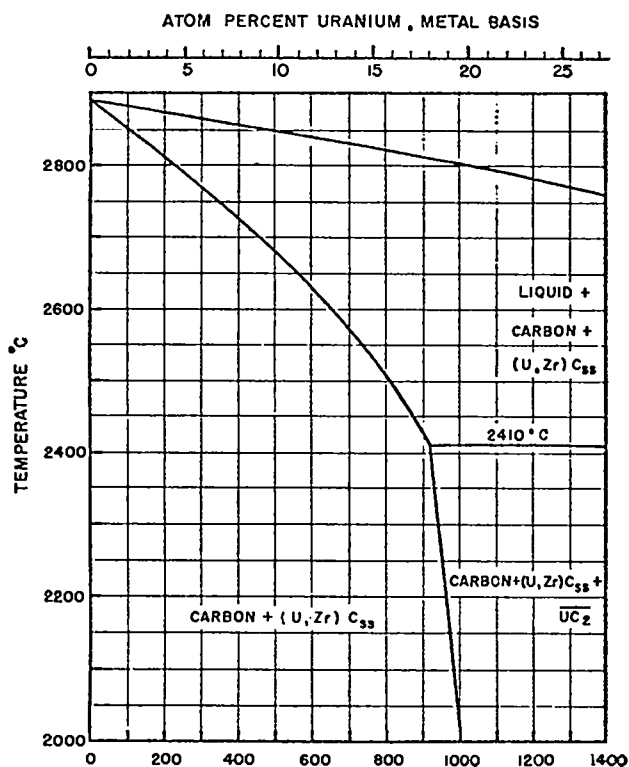


Fig. 37.  
Phase diagram for 35 vol% carbide.

~780 Mg of uranium/m<sup>3</sup> for 30 vol% carbide and at ~920 Mg for 35 vol%. This difference suggests that 35 vol% carbide composite elements can have 100- to 150-Mg/m<sup>3</sup> higher uranium loadings than 30 vol% elements before appreciable quantities of residual UC<sub>2</sub> are found.

The composite fuel element thermal stress resistance was of primary importance. As noted above, the final graphitizing temperature was a key factor in fuel element performance. The optimum temperatures for specific uranium loadings and total carbide volumes would allow 10-20% of the carbide to liquify and coalesce into a strong, interconnected network. Metallography of composite fuel element structures showed very significant changes as a function of graphitizing temperature. A metallographic structure approximating that of No. 3 in Fig. 38 was selected as part of the fuel element specification. In addition to providing continuous carbide and graphite networks, it increased the fuel element thermal conductivity from 50 W/m·K at room temperature for a low-temperature (no liquid phase) graphitized structure to 90 W/m·K for the optimum structure. Structures obtained at still higher graphitizing temperatures (more liquid

phase) had thermal conductivities of 140 W/m·K, but the mechanical properties were very badly degraded. The increased thermal conductivity is attributed to the ordering of the crystallites in the graphite flour particles and binder carbon, aided by the presence of the liquid carbide. The continuity of the carbide network was demonstrated by leaching a 35 vol% composite fuel element in hot hydrogen to remove the free carbon. The resulting structure retained the shape and dimensions of the starting fuel element, although the compressive strength had decreased ~90%.

The general characteristics of composite fuel elements are summarized in Table IV. Table V lists the typical chemical analyses of a composite element of three different uranium contents. The effects of 15-45 vol% carbide on the chemistry and structure of composite elements containing two different uranium loadings are noted in Table VI. Table VII shows the stability of ZrC-coated composite elements during long-term storage.

We made several experimental composite fuel elements from graphite flours ground from high-CTE graphite stock. We wanted to produce an element whose CTE approached that of the ZrC coating (7.7 μm/m·K) to minimize or eliminate coating cracks. Coatings deposited on matrices with a CTE of 6.1 μm/m·K had formed ~600 circumferential cracks per meter of length, whereas those on matrices with CTEs > 6.5 μm/m·K were crack-free. Crack-free coated fuel elements were expected to show very low carbon losses during high-temperature reactor testing.

Commercial high-CTE graphite flours KX-88, JM-15, GL-1076, and POCO (low-fired), were evaluated in composite elements. At uranium loadings below 400 Mg/m<sup>3</sup>, none of these element CTEs exceeded 6.8 μm/m·K after optimum graphitization heat treatment. All were substantially higher, however, than those of elements made with the standard S97 graphite flour. At 725-Mg/m<sup>3</sup> uranium loadings, the final CTEs were 7.0-7.2 μm/m·K, higher than those of any previous fuel elements. Matrices made with high-CTE flours were more isotropic than those made with the standard S97 graphite flour.

The experimental composite elements tested in NF-1 confirmed the belief that minimizing the thermal expansion mismatch between the coating and fuel element matrix would reduce coating cracks and carbon mass loss. Twenty-four composite elements with a CTE of 6.1 μm/m·K had an average carbon loss of 37.6 g per element as compared to 13.7 g per element for the 23 fuel elements with a CTE ≥ 6.5 μm/m·K, a > 60% reduction. However, a new factor

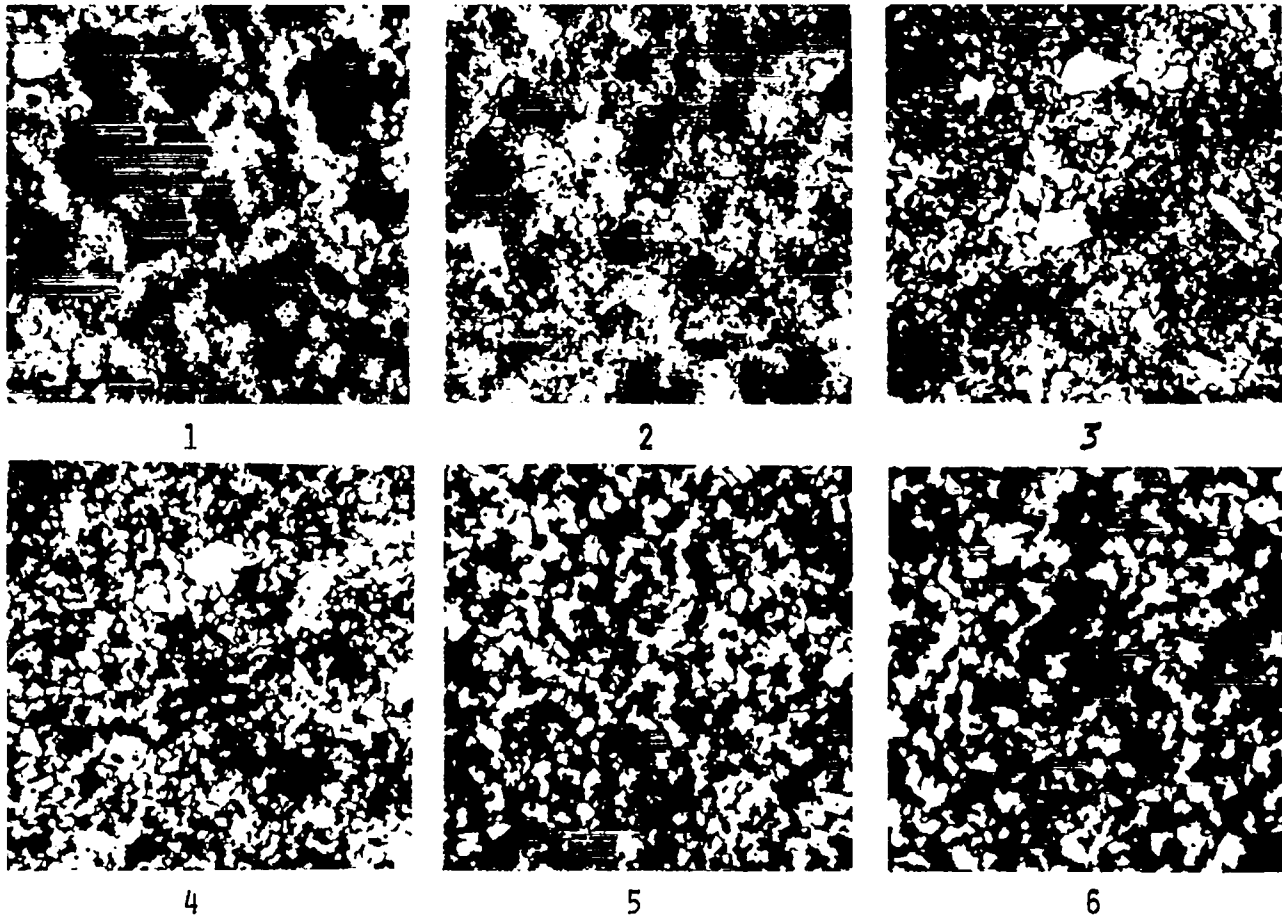


Fig. 38.  
Metallographic-structure rating system.

TABLE IV

GENERAL CHARACTERISTICS OF (U,Zr)C GRAPHITE  
COMPOSITE FUEL ELEMENTS

Parameter	Value
Carbide content (vol %)	30 - 35
Useful U-loading range ( $Mg/m^3$ )	50 - 650
Thermal conductivity at 300 K ( $W/m \cdot K$ )	50 - 90
CTE at 293-2300K ( $\mu m \cdot K$ )	6 - 7
Flexural strength at 300 K (MPa)	~ 50
Compressive strength at 300 K (MPa)	~110
Strain to fracture at 300 K ( $\mu m/m$ )	2000 - 3000
Stress at fracture at 300 K (MPa)	35 - 50
Elastic modulus at 300 K (GPa)	~ 50
Compressive deformation at 2800 K and 3.5 MPa for 1 h (%)	0.5-1.0
Thermal stress resistance at ~1700 K (power density at fracture)( $MW m^{-3}$ )	4500 - 6000

TABLE V

CHEMICAL ANALYSIS OF COMPOSITE  
FUEL ELEMENT MATRICES

Parameter	Uranium Loading ( $Mg/m^3$ )		
	180	399	598
U (wt%)	5.2	11.1	16.4
Zr (wt%)	56.0	52.5	49.6
C (wt% total)	38.8	36.0	33.6
Density ( $Mg/m^3$ )	3.49	3.61	3.64
Carbide content (vol%)	34.9	35.5	35.6
U on a metal basis (at.%)	3.5	7.6	11.4

**TABLE VI**  
**CHEMICAL CONTENT AND DENSITY OF (U,Zr)C GRAPHITE**  
**COMPOSITE FUEL ELEMENTS**

Parameter	~70-Mg/m <sup>3</sup> Uranium Loading			~435-Mg/m <sup>3</sup> Uranium Loading			
	Nominal Carbide Content (vol%)			Nominal Carbide Content (vol%)			
	15 <sup>a</sup>	20	30	30	35	40	45
Gross density (Mg/m <sup>3</sup> )	2.62	2.82	3.26	3.36	3.39	3.87	4.09
Zirconium (wt%)	34.0	40.7	52.9	46.6	51.0	56.0	59.7
(Mg/m <sup>3</sup> )	0.89	1.15	1.72	1.56	1.83	2.17	2.44
Uranium (wt%)	2.7	2.58	2.22	12.50	12.02	11.22	10.65
(Mg/m <sup>3</sup> )	70.0	72.8	72.4	420	431	435	436
Carbon (wt%)	63.3	56.4	44.8	40.5	36.5	32.6	29.2
(Mg/m <sup>3</sup> )	1.66	1.59	1.46	1.36	1.31	1.26	1.20
Carbide (vol%) <sup>b</sup>	15.0	20.2	30.1	30.5	35.2	41.0	45.5
Carbon (vol%) <sup>b</sup>	73.3	68.4	58.6	54.0	49.8	45.5	40.5
Voids (vol%) <sup>b</sup>	11.7	11.4	11.3	15.5	15.0	13.5	14.0
ZrC (wt%)	38.4	46.1	59.7	52.7	57.7	63.4	67.6
UC (wt%)	2.8	2.7	2.4	13.1	12.6	11.8	11.2
Free C (wt%)	58.5	59.9	37.7	33.7	29.2	24.7	20.8

<sup>a</sup>Estimated.

<sup>b</sup>The carbon density was assumed to be 2.1 Mg/m<sup>3</sup> rather than the 2.26 of crystalline graphite. The densities of ZrC<sub>0.97</sub> and UC<sub>0.97</sub> were assumed to be 6.59 and 13.60 Mg/m<sup>3</sup>, respectively. The density of (U,Zr)C<sub>0.97</sub> was assumed to be proportional to the mole fraction of the carbide constituents.

**TABLE VII**  
**CHANGES IN (U,Zr)C GRAPHITE FUEL ELEMENTS<sup>a</sup>**  
**AFTER STORAGE FOR 6 AND 12 MONTHS**

Parameter	Dry Storage <sup>b</sup>		Wet Storage <sup>c</sup>	
	6 Mo	12 Mo	6 Mo	12 Mo
Electrical resistance (%)	-0.6	-0.2	+1.9	+2.4
Mass change (%)	0.0	0.0	+0.4	+0.5
Dimensional change across flats (%)	+0.0012	+0.0011	+0.0012	+0.0016

<sup>a</sup>30 vol%, uranium contents 125-500 Mg/m<sup>3</sup>.

<sup>b</sup>Storage at ambient temperature in nitrogen containing Linde Molecular Sieve 4A desiccant.

<sup>c</sup>Storage in air at 310 K and 90% RH.

in these test results, radiation damage in the colder section of the element, accounted for the higher-than-anticipated mass losses in the high-CTE composite elements. Apparently, interaction of fission fragments with the graphite degraded the thermal transport properties of the matrix and the resulting temperature gradients cracked the ZrC coating. The composite fuel elements, however, withstood peak power densities of 4500-5000 MW/m<sup>3</sup> without major difficulties. We concluded that such elements would perform satisfactorily for at least 2 h, and possibly 4 to 6 h, in a nuclear propulsion reactor that heated hydrogen gas to 2500-2800 K.<sup>33</sup>

### C. Carbide Elements

Development of a carbide fuel element for a very high temperature, 3200 K (2927°C), nuclear rocket engine was not undertaken until late in the Rover program, and only limited effort, compared to previous fuel element work, was actually expended. The incentive for developing such an element was the possibility of operating a reactor core for a long time at as high as 3200 K (2927°C), equivalent to a specific impulse of 950 s. There would be no serious loss of carbon, uranium, or zirconium from such a fuel element, and no coating problem.

The carbide fuel element concept called for an entirely new design philosophy. Whereas all previous 19-hole, 1321-mm (52-in.) -long elements were developed to withstand high thermal stresses without cracking, to prevent carbon loss from the cracked areas in a hot hydrogen environment, the carbide concept accepted fuel breakage. Carbides have poor thermal stress resistance, but, even if the fuel element cracked during the reactor run, there would be no carbon loss problem. The major area of concern was possible crumbling of the carbide fuel element into particles that would block passage of the hydrogen gas.

The carbide fuel element reactor core concept envisaged thousands of small-bore, 3.2-mm (0.128-in.); hexagonal, 5.5 mm (0.22 in.) across flats; half-length, 0.64 m (25.6 in.), elements stacked together to build up the core length and diameter. Two of the 49 individual cells in NF-1 contained carbide elements; each contained 7 elements bundled together and another 7 on top to achieve the desired length. Three types of matrix experiments were included in these test elements.

The carbide fuel elements were extruded with a circular cross section out of a small 40-ton laboratory extrusion press from a mix consisting of ZrC, enriched UO<sub>2</sub> and ZrO<sub>2</sub> powders, graphite flour, and Varcum binder, all of reactor-grade purity. The mix composition was calculated so that 3% excess carbon

remained after all the oxides had been converted to carbides. This excess carbon kept the element from sticking to graphite heating fixtures and aided in the machining operations. The low-temperature heat treatments involved heating rates and temperatures like those for other Varcum-bonded fuel elements. Argon atmospheres were used in all heat treatments to prevent oxidation of the carbides. At the higher heat treatment temperatures, the individual carbide tubes were held in graphite cassettes and taken slowly through the temperature regime in which the oxides were converted to carbide. The final high-temperature heat treatment was ~2800 K (2527°C) for 2 h.

The heat-treated carbide tubes were centerless ground and then diamond-milled into hexagons. The bores were not machined. The hexagonal elements, containing 3% excess carbon, were then heated in flowing hydrogen at 2300 K (2027°C) to remove the available free carbon in the carbide structure and then CVD impregnated with zirconium at 1900 K (1627°C). The three experimental carbide matrices in NF-1 were impregnated with 0, 3, and 8% zirconium, respectively, in this treatment. A final 2-h heat treatment at 2800 K (2527°C) yielded a substoichiometric carbide with a carbon:metal atom ratio of 0.8:0.92. Table VIII shows the general characteristics of the carbide fuel elements tested in NF-1.

These elements were tested to determine their fracture mode. There were many transverse and some longitudinal fractures, but no fragmentation into small particles. The 8% impregnated carbide elements were not so fractured as the other two types.

The design and fuel element development effort for a carbide core reactor was minimal, and much could be done to improve the element behavior and minimize the thermal stresses during reactor operation. An improved matrix coupled with a modified design would increase the fracture resistance of carbide elements significantly. The very high temperature capability of these elements in a hydrogen environment provides a unique capability for future reactor concepts.

## XII. FUEL ELEMENT PROPERTIES

The Rover and NERVA fuel elements were essentially a ceramic, and the reactor designers tailored their design requirements around this brittle material. The elements were designed for compressive loading during reactor operation, and bending stresses were also considered. Most of the mechanical property evaluation, therefore, involved

**TABLE VIII**  
**GENERAL CHARACTERISTICS FOR (U,Zr)C**  
**CARBIDE FUEL ELEMENTS**

Parameter	Impregnation Mass Gain (%)		
	0	3	8
Uranium loading (Mg/m <sup>3</sup> )	~300	~300	~300
U (%)	5.88	5.64	5.42
Zr (%)	82.9	83.1	83.5
Total C (%)	11.0	11.0	10.8
Free C (%)	<0.05	<0.05	<0.05
O (%)	0.05	0.07	0.04
N (%)	0.14	0.22	0.29
Carbon: metal atom ratio	0.981	0.980	0.958
Density (Mg/m <sup>3</sup> )	5.48	5.46	5.71
Porosity (%)	23	21	18
Thermal conductivity <sup>a</sup> (W/m·K)	10.0	8.6	8.2
Long/Trans properties <sup>a</sup>			
Failure strain (μm/m)	540/460	470/460	300/450
Failure stress (MPa)	140/75	140/90	100/95
Modulus (GPa)	250/160	290/200	300/210
CTE <sup>b</sup> (μm/m·K)	7.8	7.8	7.8
Compressive deformation <sup>c</sup> (%)			
at 2770 K	---	4	2
at 2870 K	---	---	5
at 2970 K	26	20	7

<sup>a</sup>Room temperature longitudinal and transverse properties.

<sup>b</sup>CTE, 293-2300 K.

<sup>c</sup>6.9 MPa for 1 h.

procedures like those used for brittle materials, specifically, a deflection test. Although the data were obtained on a sample of elements produced for reactor cores, no element failed to meet the specification of 24.1-MPa (3500-psi) flexural strength or 69-MPa (10 000-psi) compressive strength. Consequently, mechanical properties were never considered the villain in any reactor core problems that involved graphitic fuel elements.

The thermal stress characteristics of a fuel element are influenced by such factors as elastic modulus, CTE, thermal conductivity, and strength. Consequently, these data were accumulated for the thermal stress testing program. Thermal conductivity data also were desired for reactor calculations. Fuel element permeability was measured, but its value relative to reactor operation probably is questionable.

The limited property data accumulated during most of the Rover and NERVA program was interesting, but much of it was not significantly applicable to fuel element performance in reactor cores. The CTE problem that caused cracks in the NbC coating was recognized early and led to the effort to obtain high-CTE graphite flour for making fuel elements. It was really the impetus from the thermal stress testing of composite and high-CTE graphite elements in the late 1960's that focused increased attention on how fuel element properties affected their behavior. Graphite matrix elements loaded with UO<sub>2</sub> or coated particles and made with the available low-CTE graphite flours had extremely good thermal stress characteristics and were difficult to break in a thermal stress test. Consequently, only minimal property data was obtained on these elements. Introduction of the high-CTE graphite

and carbide and graphite composite element with completely different thermal stress characteristics led to increased acquisition of data on composite elements. A large volume of property data was included in LASL internal documents from Groups N-1 and N-7 but, unfortunately, only a small amount was issued in reports.

### A. Unfueled Graphite

The data in Table IX are typical property information collected on unfueled components for reactor cores.

### B. Fueled Graphite

Table X lists some of the property data on 19-hole, KIWI-B type elements fueled with  $UO_2$ .

TABLE IX

#### UNFUELED GRAPHITE EXTRUSIONS

Density	1.8-1.9 Mg/m <sup>3</sup>
Flexural strength (RT) <sup>a</sup>	40.1 ± 2.65 MPa (5890 ± 385 psi)
Flexural strength (2773 K)	73.4 MPa (10 640 psi)
Compressive strength (RT)	85.4 ± 4.3 MPa (12 385 ± 625 psi)
Modulus of elasticity	6.9-10.3 GPa (1-1.5 psi)
Strain to failure	2000-4000 μm/in.
CTE	2-4 μm/m·K (293-2273 K)

<sup>a</sup>RT = room temperature.

Table XI lists mechanical property data acquired from elements containing coated particles during fabrication of the Phoebus 1 and 2 and Pewee-1 reactor cores.

We prepared a series of single-hole tube extrusions for which we added varying amounts of NbC powder to the basic graphite flour composition. The S97 flour was the same as that used in extrusion of coated-particle loaded elements, and the 0.6 μm-flour was a finer grind of the same flour. Table XII lists the measured physical and mechanical properties of these extrusions.

The data in Table XIII were collected to evaluate the strength of composite (40 wt% TaC-40 wt% NbC-20C) tip material brazed to unfueled and fueled graphite extrusions.

### C. Composite Fuels

The significantly different thermal stress characteristics of the (U,Zr)C-graphite composite fuel elements led to a much greater effort to determine properties of interest for the various composite materials. The results of many tests on composite fuel elements of varying carbide and/or uranium content are included in the following tables.

Table XIV shows how carbide content affects the mechanical properties of composite fuel elements.

Table XV shows how carbide content affects the modulus of composite fuel elements.

The high-temperature deformation of composite fuel elements of varying carbide and uranium content is indicated in Table XVI.

TABLE X

#### OXIDE-LOADED KIWI-B FUEL ELEMENTS

Uranium Loading (Mg/m <sup>3</sup> )	Carbon Density (Mg/m <sup>3</sup> )		
	Max	Min	Avg
343	1.809	1.737	1.777
298	1.821	1.776	1.800
261	1.832	1.7912	1.805
226	1.848	1.813	1.829
189	1.847	1.811	1.828
Flexural strength (RT)	~34.5 MPa (5000 psi)		
Compressive strength (RT)	~68.9 MPa (10 000 psi)		
Tensile strength (RT)	20.7 MPa (3000 psi)		
Ultimate strain to failure	25.000-3000 μin./in.		
Modulus of elasticity	13.8 GPa (2 x 10 <sup>6</sup> psi)		

TABLE XI

## FUEL ELEMENT LOADED WITH COATED PARTICLES

Uranium Loading (Mg u/m <sup>3</sup> )	Compressive Strength, MPa (psi)	Flexural Strength, MPa (psi)
193 ± 84 <sup>a</sup>	90.66 ± 5.92 (13 150 ± 860)	39.61 ± 6.65 (5745 ± 965)
220 ± 75 <sup>b</sup>	93.35 ± 4.34 (13 540 ± 630)	30.13 ± 2.21 (4370 ± 320)
450	88.94 ± 4.13 (12 900 ± 600)	29.30 ± 0.58 (4251 ± 85)
750	73.15 ± 2.50 (10 610 ± 363)	31.57 ± 0.70 (4580 ± 100)
999	70.32 ± 0.98 (10 200 ± 142)	29.44 ± 1.86 (4270 ± 270)
Pewee-1 <sup>c</sup>	85.28 ± 4.34 (12 370 ± 630)	34.95 ± 3.45 (5070 ± 500)

<sup>a</sup>Average of Phoebus 2A elements with 2.79-mm-diam boreholes.

<sup>b</sup>Average of Phoebus 1C elements with 2.54-mm-diam boreholes.

<sup>c</sup>Average of Pewee-1 production; uranium loading, 126-525 Mg/m<sup>3</sup>.

An attempt to evaluate how leaching of carbon from a fuel element affects compressive deformation is shown in Table XVII.

Table XVIII shows the matrix properties of composite fuel elements tested in NF-1, and Table XIX compares the thermal conductivities of several materials.

The composite fuel elements for the NF-1 reactor test were prepared from several different graphite flours. Table XX indicates some of the properties shown by representative elements of each type. It also shows the relative thermal conductivities of composite materials as a function of heat treatment and of graphite and ZrC content.

TABLE XII

## PROPERTIES OF EXTRUDED NbC-C COMPOSITES

## PHYSICAL

Nominal vol% Carbide	Filler Carbon	Density (Mg/m <sup>3</sup> )			Electrical Resistivity at 20° (Ω/cm x 10 <sup>-6</sup> )	CTE (μm/m·K) at 293-2273 K		Dynamic Modulus at 293 K (GPa)
		Theoretical	Calculated	Immersion		Across Grain	With Grain	
10	S-97	2.39	2.46	2.48	927	5.71	4.30	22.06
20	S-97	3.62	3.02	3.05	584	6.19	5.35	25.44
30	S-97	4.39	3.68	3.70	317	6.73	6.25	35.71
40	S-97	5.12	4.25	4.27	183	7.23	6.80	48.81
40	(0.6 μm)	5.15	4.10	4.32	239	7.21	---	---

## MECHANICAL

Flour	NbC (Vol%)	Density (Mg/m <sup>3</sup> )	Flexural Strength, MPa (psi)	Elastic Modulus, GPa (x 10 <sup>6</sup> psi)	90-min Compressive Deformation (%)	
					Cycle <sup>a</sup>	Single-Point <sup>b</sup>
S-97	10.2	2.406 ± 0.007	45.23 ± 4.20 (6 560 ± 610)	11.16 (1.62 ± 0.05)	0.80	0.08
S-97	20.9	2.961 ± 0.006	57.70 ± 1.79 (8 370 ± 260)	12.06 (1.75 ± 0.05)	0.10	0.08
S-97	32.6	3.613 ± 0.006	69.91 ± 2.58 (10 140 ± 375)	18.48 (2.68 ± 0.21)	0.15	0.18
S-97	43.1	4.111	74.80 (10 850)	21.44 (3.11)	0.20	0.20
0.6 μm	43.9	3.940 ± 0.012	77.05 ± 1.79 (11 175 ± 260)	23.51 (3.41 ± 0.15)	0.10	0.00

<sup>a</sup>Nine 10-min cycles at 2773 K and 3.44 MPa.

<sup>b</sup>One 90-min cycle at 2773 K and 3.44 MPa.

TABLE XIII

FLEXURAL STRENGTH OF MOLYBDENUM-BRAZED COMPOSITE TIP JOINTS

Matrix	Test Temp	Flexural Strength, MPa (psi)	Fracture Location
Unfueled graphite	Room temp	26.6 (3860)	Matrix
Unfueled graphite	Room temp	20.6 (2990)	Matrix
Unfueled graphite	2773 K (He)	24.3 ± 2.93 (3520 ± 425)	Joint
Unfueled graphite <sup>a</sup>	2773 K (He)	36.33 ± 5.3 (5270 ± 770)	Joint
Bead-loaded	2773 K (He)	26.40 ± 1.8 (3830 ± 260)	Joint
Bead-loaded <sup>b</sup>	2773 K (He)	25.9 (3760)	Joint
Bead-loaded <sup>c</sup>	2773 K (He)	5.7 (825)	Joint

<sup>a</sup>After hot-gas testing in hydrogen at 1823-2498 K.

<sup>b</sup>After three 20-min hydrogen cycles at 2333 K.

<sup>c</sup>After three 20-min hydrogen cycles at 2498 K.

TABLE XIV

ROOM-TEMPERATURE FLEXURAL, COMPRESSIVE, AND TENSILE FRACTURE STRENGTHS OF (U,Zr)C GRAPHITE FUEL ELEMENTS

Carbide Content (vol%)	Strength <sup>a</sup> (MPa)		
	Flexural	Compressive	Tensile
10	44.8 ± 2.7	74.5 ± 0.7	35
20	47.9 ± 1.4	97.6 ± 1.8	43
25	63.4 ± 5.1	109.5 ± 12.4	49
30	53.0 ± 1.6	118.1 ± 10.3	39
50	65.6 ± 2.3	>290	68
Pewee-1 graphite elements	35.0 ± 3.4	85.3 ± 4.3	---

<sup>a</sup>Average of at least three samples of full cross section, ~19 mm across flats. The flexural and tensile strengths were transverse to the extrusion direction; the compressive strengths, parallel.

XIII. SUMMARY

Creating fuel elements for nuclear rocket engines presented a unique challenge to materials development workers. Reactor fuel elements had never been operated at temperatures up to 2773 K (2500°C) in a hydrogen environment, and the technical problems

TABLE XV

ROOM-TEMPERATURE ELASTIC MODULUS

Carbide Content (vol%)	Longitudinal Elastic Modulus <sup>a</sup> (GPa)	Transverse Effective Elastic Modulus <sup>b</sup> (GPa)	Modulus Ratio Long/Trans
10	17.6	5.9	3.0
20	25.4	7.9	3.2
25	30.3	9.6	3.2
30	42.0	11.8	3.6
50	108.0	44.0	2.5

<sup>a</sup>Dynamic method.

<sup>b</sup>Load-deflection method.

TABLE XVI

COMPRESSIVE DEFORMATION OF (U,Zr)C GRAPHITE COMPOSITE ELEMENTS SUBJECTED TO 3.45 MPa FOR ONE HOUR

Carbide Content (vol%)	Uranium Loading (Mg/m <sup>3</sup> )	Compressive Deformation (%)			
		2773 K	2873 K	2923 K	2973 K
10	300	0.22	0.21	0.26	0.20
20	300	0.43	1.02	1.08	1.10
25	300	0.37	0.50	0.59	0.61
30	300	0.72	0.98	1.45	2.35
30	500	0.41	0.43	---	---
40	500	0.76	0.87	---	---
50	300	0.8	3.1	5.1	11.1
50	500	2.5	2.6	---	---

TABLE XVII

COMPRESSIVE DEFORMATION OF PARTIALLY LEACHED,<sup>a</sup> SOLID, 30 vol% ZrC STOCK STRESSED TO 500 PSI (3.45 MPa) FOR ONE HOUR AT TEMPERATURE

Element	Temp (°C)	Compressive Deformation ΔL/L (%)
Leached	1500	0.81 ± 0.15
Unleached	1500	0.01 ± 0.01
Leached	2000	1.70 ± 0.94
Unleached	2000	0.04 ± 0.02
Leached	2250	3.35 ± 0.17
Unleached	2250	0.00 ± 0.03

<sup>a</sup>Leached in hydrogen for 10 min at 2100°C to remove carbon; leaching incomplete.

TABLE XVIII

MATRIX PROPERTIES OF COMPOSITE ELEMENTS IN THE NF-1 REACTOR

Carbide Content (vol%)	Thermal <sup>a</sup> Expansion (μm/m·K)	Thermal Conductivity <sup>b</sup> (W/m·K)	Fracture Power Density (MW/m <sup>3</sup> )
35	6.7	75	4700
35	6.7	74	4900
35	6.6	71	5000
35	6.6	84	5200
35	6.8	80	5400
35	6.8	87	6100
30	6.5	83	5500
30	6.5	77	5800
30	6.6	75	6200
30	6.1	40-50	4700-5500

<sup>a</sup>293-2300 K.

<sup>b</sup>At ~300 K.

were, indeed, formidable. The task was accomplished successfully, fuel elements performed for several hours under extreme reactor conditions, and significant technical accomplishments were achieved.

TABLE XIX

THERMAL CONDUCTIVITY OF ATJ-S GRAPHITE, ZrC CARBIDE, AND TWO(U,Zr)C GRAPHITE COMPOSITES

Temp (K)	Thermal Conductivity (W/m·K)			
	Composite A <sup>a</sup>	Composite B <sup>b</sup>	ATJ-S	ZrC
300	52	90	125	19
400	49	71	110	20
500	46	60	97	20.5
600	43	53	86	21
700	40	48	78	21.5
800	38	44	72	22
1000	34	38	60	23.5
1200	32	36	52	25
1400	30	30	45	27
1600	30	30	41	29
1800	30	30	38	31
2000	30	30	35	33
2200	30	30	33	35
2400	30	30	32	36
2600	30	30	30	38

<sup>a</sup>Heat-treated at temperatures below the solidus line.

<sup>b</sup>Optimum heat-treatment conditions for this composition.

ed. New and extremely promising materials for prolonged high-temperature operation were being evaluated when the program was stopped.

This overview of the entire fuel element development program is presented to make the history of the accomplishment available for new undertakings with high-temperature fuels. No specific topic could be discussed extensively, but the references should guide anyone wishing to pursue the high-temperature fuel element problem.

The Rover and NERVA nuclear engine program was extremely successful technically. There is no doubt that a nuclear rocket engine is feasible. The program was cancelled because no US agency had a specific mission that required a nuclear rocket engine.

REFERENCES

1. R. Serber, "The Use of Atomic Power for Rockets," Douglas Aircraft Company (July 1946).

**TABLE XX**  
**THERMAL-STRESS RESISTANCE OF UNCOATED COMPOSITE ELEMENTS**

Extrusion Lot	Filler Flour	Carbide Content (vol%)	CTE at (293-2300 K) ( $\mu\text{m}/\text{m}\cdot\text{K}$ )	Room-Temp Thermal Cond <sup>a</sup> ( $\text{W}/\text{m}\cdot\text{K}$ )	Fracture Power Density ( $\text{MW}/\text{m}^3$ )		
					G	M	H
17	AXM <sup>b</sup>	Graphite <sup>c</sup>	5.6	---	4050	4500	4500
8 <sup>d</sup>	GL-1074 <sup>e</sup>	30	6.6	75H	6200	5500	>6300
68	S-97 <sup>f</sup>	30	6.1	61H	6600	6600	6600
65	KX-88	30	6.5	62M, H	4300	4700	5500
65	KX-88	30	6.5	93G, 68H	>6700	5100	5300
713	S-97	35	6.3	50G, M, H	4700	>6200	>5300
54	KX-88 <sup>f</sup>	35	7.0	49M, H	4000	3700	3500
62	KX-88	35	6.6	71M, H	5200	5100	4400
60	KX-88	35	6.6	85M, H	5000	>6900	5300
50	KX-88	35	6.8	81M, H	5400	5300	5200
62	KX-88	35	6.8	87M, H	6800	6000	5800
53	JM-15 <sup>f</sup>	35	6.7	75M, H	3700	5200	5000
56	JM-15/KX-88	35	6.7	76M, H	5100	4600	4800

<sup>a</sup>G, M, and H indicate low-, medium-, and high-temperature stations along fuel element length.

<sup>b</sup>Product of POCO Graphite Company.

<sup>c</sup>A graphite matrix element containing pyrocarbon-coated UC<sub>2</sub> particles.

<sup>d</sup>Composite elements fabricated by WANL.

<sup>e</sup>Product of Great Lakes Carbon Company.

<sup>f</sup>Product of Speer Carbon Company.

2. R. Cornog, "Rocket Computations," General Electric Company report NEPA-508 (August 3, 1946).

3. R. E. Adams, "An Estimate of Nuclear Rocket Performance," General Electric Company report NEPA-283 (September 15, 1947).

4. A. V. Cleaver and L. R. Shepherd, "The Atomic Rocket I, II, III, and IV," Brit. Interplanet. Soc. (September 1948, November 1948, January 1949, and March 1949).

5. E. P. Carter, "The Application of Nuclear Energy to Rocket Propulsion, A Literature Search," Oak Ridge National Laboratory report ORNL. Y-93 (December 29, 1952).

6. R. W. Bussard, "Nuclear Energy for Rocket Propulsion," AEC report TID-2011 (December 1953).

7. R. L. Aamodt and George Bell, "The Feasibility of Nuclear-Powered Long Range Ballistic Missiles," Los Alamos Scientific Laboratory report LAMS-1870 (March 1955).

8. R. E. Schreiber, "The LASL Nuclear Rocket Propulsion Program," Los Alamos Scientific Laboratory report LAMS-2036 (April 1956).

9. H. Gordon and T. C. Merkle, "Nuclear Rocket Symposium," University of California, Livermore report COPP-1851 (January 1957).

10. D. H. Schell, J. W. Taylor, and J. M. Taub. "Fabrication of Fuel Elements for the KIWI-A Reactor," Los Alamos Scientific Laboratory report LA-2418 (March 1960).
11. M. C. Tinkle, W. J. McCreary, B. D. Travis, R. J. Bard, and J. A. Kricher, "Preparation of Minus 10 Micron Dense  $UO_2$ ," Los Alamos Scientific Laboratory report LA-2521 (July 1960).
12. J. C. Bokros, "Structure of Pyrolytic Carbon Deposited in a Fluidized Bed," Carbon 3, 17 (1965).
13. R. J. Bard, H. R. Baxman, J. P. Bertino, W. J. McCreary, et al., "Development of Particles Coated with Pyrolytic Carbon," Los Alamos Scientific Laboratory reports LA-3496 (January 1967), LA-3601 (March 1967), LA-3660 (June 1967), LA-3767 (February 1968), LA-3984 (November 1968), LA-4139 (May 1969), LA-4226 (November 1969), and LA-4308 (December 1969).
14. A. W. Savage, Jr., R. C. Feber, J. P. Bertino, H. R. Baxman, J. A. O'Rourke, and R. J. Bard. "Development of ZrC-Coated UC-ZrC Particles." Los Alamos Scientific Laboratory report LA-4005 (January 1969).
15. D. H. Schell, J. W. Taylor, and J. M. Taub. "Fabrication of Uranium-Loaded Graphite," Los Alamos Scientific Laboratory report LAMS-2587 (July 1961).
16. W. W. Martin, D. H. Schell, J. M. Taub, and J. W. Taylor, "The Fabrication of Uranium-Loaded Graphite Fuel Elements for KIWI-B4/B5 Rockets," Los Alamos Scientific Laboratory report LA-2936 (June 1963).
17. D. Pavone, "Some Experiments Concerned with the Reaction Between  $UO_2$  and Graphite," Los Alamos Scientific Laboratory report LA-2096 (September 1956).
18. A. M. Zerwas and F. E. Stack, "Machining and Inspection Procedures Used at Los Alamos Scientific Laboratory for Fuel Elements of the KIWI-B4 Series," Los Alamos Scientific Laboratory report LA-2669 (February 1962).
19. D. C. Winburn, R. K. Money, Roy Krohn, C. P. Gutierrez, G. H. Moulton, M. G. Bowman, and D. T. Vier, "Carbide Protective Coatings on Graphite Fuel Elements for KIWI-A Prime and KIWI-A3," Los Alamos Scientific Laboratory report LAMS-2646 (September 1961).
20. D. C. Winburn, R. K. Money, Roy Krohn, W. L. Drumhiller, and M. G. Bowman, "NbC Cladding of Bores and NbC Vapor Coating of Ends of Uranium-Loaded Graphite Fuel Elements for KIWI-B1A," Los Alamos Scientific Laboratory report LAMS-2668 (January 1962).
21. A. J. Caputo, "NERVA Fuel Element Development Program Summary Report—July 1966 through June 1972: Vapor Deposition of Metal Carbides," Union Carbide Oak Ridge Y-12 Plant report Y-1852. Part 4 (1972).
22. A. J. Caputo, "NERVA Fuel Element Development Program Summary Report—July 1966 through June 1972: Characterization of Vapor Deposited Niobium and Zirconium Carbides," Union Carbide Oak Ridge Y-12 Plant report Y-1852, Part 3 (1972).
23. G. H. Tenney and members of Group GMX-1, "The Role of Nondestructive Testing in the Rover Fuel Element Program," Los Alamos Scientific Laboratory report LA-2672 (February 1962).
24. B. L. Blanks. "Nondestructive Testing of Graphite at the Los Alamos Scientific Laboratory," ASTM Special Technical Publication No. 439. 1968. p. 18.
25. R. M. Ford and R. D. Strong, "Masked Eddy Current Probe for Detection of Rover Fuel Element Coating Cracks," Los Alamos Scientific Laboratory report LA-4590-MS (February 1971).
26. M. A. Winkler and H. J. Fulbright, "Improved Method of Fuel Element Incremental Mass Measurement," Los Alamos Scientific Laboratory report LA-4105 (December 1969).
27. H. C. Nicholson and L. L. France, "Joining of Graphite Fuel Elements for the NRX-B Advanced Design." Westinghouse Astronuclear Laboratory report WANL-TME-847 (July 1964).
28. D. J. Sandstrom, "Joining Graphite to Graphite with Transition Metal Foils," Los Alamos Scientific Laboratory report LA-3960 (July 1968).
29. J. C. Rowley, W. R. Prince, and R. G. Gido, "A Study of Power Density and Thermal Stress Limitations of Rover Reactor Fuel Elements," Los

Alamos Scientific Laboratory report LA-3323-MS (July 1965).

30. F. J. Witt, "Graphite Mechanics Program-Progress Report No. 7," Oak Ridge National Laboratory report CF 66-4-69 (April 1966).

31. B. L. Greenstreet, "Fracture of Graphite," Quarterly Progress Reports; Union Carbide Corporation—Nuclear Division, Oak Ridge National Laboratory. Oak Ridge, TN, July 1969 through 1971.

32. W. R. Prince and R. G. Lawton. "Rover Graphite Fuel Element Thermal Stress Experiments and Analyses," Los Alamos Scientific Laboratory report LA-3849-MS (July 1968).

33. L. L. Lyon, "Performance of (U,Zr)C-Graphite (Composite) and of (U,Zr)C (Carbide) Fuel Elements in the Nuclear Furnace I Test Reactor." Los Alamos Scientific Laboratory report LA-5398-MS (September 1973).

34. J. M. Napier, "NERVA Fuel Element Development Program Summary Report July 1966 through June 1972: Extrusion Studies," Union Carbide Corporation Oak Ridge Y-12 Plant report Y-1852, Part I (1972).

35. K. V. Davidson, W. W. Martin, D. H. Schell, J. M. Taub, and J. W. Taylor, "Development of Carbide-Carbon Composite Fuel Elements for Rover Reactors." Los Alamos Scientific Laboratory report LA-5005 (October 1972).

## APPENDIX

### ROVER AND NERVA TESTS AT NRDS

**July 1, 1959**

The KIWI-A reactor was tested by LASL. It was operated for 5 min at 70 MW and provided important reactor design and materials information.

Uncoated,  $UO_2$ -loaded, plate-type fuel elements; gaseous hydrogen.

**July 8, 1960**

The KIWI-A prime reactor was tested by LASL. It was operated for nearly 6 min at 85 MW to demonstrate an improved fuel element design. Some core structural damage occurred.

Short, cylindrical  $UO_2$ -loaded fuel elements containing four holes; NbC-coated by CVD process; graphite modules to contain fuel elements; gaseous hydrogen.

**October 10, 1960**

The KIWI-A3 reactor was tested by LASL. It was operated for over 5 min at 100 MW. Core structural damage occurred. This experiment concluded the KIWI-A series of proof-of-principal tests which demonstrated that this type of high power density reactor could be controlled and could heat hydrogen to very high temperatures.

Same type of fuel elements as KIWI-A prime: gaseous hydrogen.

**December 7, 1961**

The KIWI-B1 reactor, first of a new series, was tested by LASL. KIWI-B reactors were designed for operation at ~1100 MW and used reflector control and a regeneratively cooled nozzle. After 30 s of operation, a hydrogen leak in the nozzle and pressure vessel interface terminated the run. The planned 300-MW maximum power was achieved as limited by the capability of the nozzle with gaseous hydrogen coolant.

Cylindrical,  $UO_2$ -loaded fuel elements ~26 in. long, containing seven holes; bores NbC-coated by tube cladding process; graphite modules to contain fuel elements; gaseous hydrogen.

**September 1, 1962**

The KIWI-B1B reactor, tested by LASL, was the first operated with liquid hydrogen. The test met its prime objective of demonstrating the ability of the system to start up and operate using liquid hydrogen feed. Following a smooth, stable start, the run was

terminated after a few seconds of 900-MW operation.

Same type of fuel elements as KIWI-B1A.

#### November 30, 1962

KIWI-B4A, the first KIWI-B design intended as a prototype flight reactor, was tested by LASL. The power run was terminated at about 50% level when bright flashes in the exhaust occurred with increasing frequency. Subsequently, intensive analyses and component testing were conducted to determine and eliminate the cause of the core damage.

Full-length,  $UO_2$ -loaded, 19-hole hexagonal fuel elements; bores NbC-coated by the tube cladding process.

#### May 15, 1963

A cold-flow version of the KIWI-B4A reactor, KIWI-B4A CF, was tested by LASL. The term "cold-flow" means that the core contained hexagonal, 19-hole, dummy fuel elements but no fissionable material and, therefore, produced no power. Otherwise, the cold flow was identical to the KIWI-B4A flow. Sixteen tests used gaseous helium and gaseous hydrogen in demonstrating conclusively that flow-induced vibrations damaged the KIWI-B4A core.

#### August 21, 1963

An improved cold-flow version of the KIWI-B4A CF reactor, KIWI-B4B CF, was tested by LASL. It was nearly identical to the KIWI-B4A CF, but contained prototype components designed to eliminate core vibration. Data from these experiments indicated that planned design improvements would eliminate structural vibrations.

#### February 13, 1964

Cold-flow tests of the redesigned reactor, KIWI-B4D, were conducted by LASL. This reactor incorporated a number of changes based on the KIWI-B4B CF results and the component test and analysis program initiated in 1963 to eliminate the destructive vibrations that occurred during the KIWI-B4A tests. The design changes were successful.

#### April 16, 1964

The NRX-A1 cold-flow reactor was tested by the Aerojet-General and Westinghouse Electric Corporations, the industrial contractor team responsible for NERVA development. This test successfully demonstrated the structural stability against flow-induced core vibration of the Westinghouse reactor design, which was based upon the LASL KIWI-B design.

#### May 13, 1964

The KIWI-B4D power reactor was tested by LASL. It operated for over 60 s at full design power with no indication of the core vibrations that destroyed KIWI-B4A. This was also the first time a completely automatic start was used for a reactor test.

Full length,  $UO_2$ -loaded, 19-hole, hexagonal fuel elements; bores NbC-coated by the tube cladding process.

#### July 28, 1964

KIWI-B4E, the eighth and final KIWI, was tested by LASL. It was operated at near full power and temperature for ~8 min, the maximum time possible with the available propellant supply.

Full-length, 19-hole, hexagonal fuel elements, loaded with coated  $UC_2$  particles; bores NbC-coated by the tube cladding process.

#### September 10, 1964

The KIWI-B4E reactor was restarted and run at near full power for ~2.5 min. Reactor rerunning capability was demonstrated for the first time. Restart is an asset in economical development of nuclear rockets.

#### September 24, 1964

The Aerojet-General and Westinghouse Electric Corporations, the NERVA engine contractor team, conducted the first power test of a NERVA experimental reactor, the NRX-A2. It was operated at ~50% of full power to ~1100-MW full power for ~5 min.

**October 15, 1964**

NRX-A2 was restarted to investigate how the hydrogen propellant affected reactor control during low-power, low-flow operation.

**January 12, 1965**

A Rover flight safety experiment, called the KIWI transient nuclear test, was successfully completed by LASL. A KIWI-B type reactor was destroyed deliberately by placing it on a very fast excursion to provide data to confirm or correct the analytical models and procedures developed.

**April 23, 1965**

NRX-A3 was operated by the NERVA industrial contractor team for a total of ~8 min. About 3.5 min was at full power.

**May 20, 1965**

NRX-A3 was restarted and run at full power for ~13 min. This was the longest single, full-power run of a nuclear rocket at that time.

**May 28, 1965**

NRX-A3 was restarted for a third power cycle and operated at low to intermediate power (up to ~45% of full power) to provide data for development of control systems and an increased understanding of intermediate power reactor dynamics. Total operating time under power was ~45 min.

**June 25, 1965**

Phoebus 1A, the first KIWI-size reactor fabricated during the Phoebus graphite reactor technology program, was tested by LASL. It was operated at full power and temperature for ~10.5 min. During shutdown from full power, exhaustion of the facility liquid hydrogen supply led to undercooling of the reactor structural components and damaged the core. This damage was not caused by reactor malfunction, but rather by a faulty Dewar level gauge that indicated adequate propellant reserves, when, in fact, the Dewar was empty.

Full-length, 19-hole, hexagonal fuel elements, loaded with coated UC<sub>2</sub> particles; bores NbC-clad by CVD process.

**March 25, 1966**

The NERVA Reactor Experimental Engine System Test (NRX-EST), which was ground tested successfully on four different days in February and March, was restarted and operated successfully again. The test was for ~15 min, of which 13.5 min were at full power (55000-lb thrust under altitude conditions or 1100-MW reactor power). It marked the end of the power testing that began February 3. During the test program, the NERVA engine system was operated at power a total of ~1 h and 50 min, of which ~28 min were at full power. These times at full power and total power were by far the greatest for a single nuclear rocket reactor at that time.

**June 23, 1966**

NRX-A5, operated successfully at full power on June 8 for ~15.5 min, was restarted and operated again at full, ~1100-MW, power for 14.5 min to bring the total operating time to half an hour. Liquid hydrogen capacity at the test facility was not sufficient to permit 30 min of continuous operation at design power.

**February 23, 1967**

Phoebus 1B was operated for ~45 min, of which 30 min, the maximum time planned, were at design power of ~1500 MW. The primary purpose was to determine how the higher power operation affected the reactor.

Same type fuel elements as Phoebus 1A.

**June 26, 1968**

Phoebus 2A operated for a total of ~32 min at significant power, ~12 min of which were at ~4000 MW. Peak power reached was ~4200 MW. The test was terminated as planned when the available propellant and water were exhausted. The reactor power density exceeded that necessary for the 75 000-lb-thrust NERVA nuclear rocket. The primary test objective was to obtain data on this advanced

reactor at intermediate and high power levels, high power density, and high-temperature operation.

Same type fuel elements as Phoebus 1A.

#### December 1968

The first Pewee reactor, Pewee-1, was tested in a series completed on December 4, 1968. One objective was to confirm the design and engineering of the reactor as a whole. Pewee-1 ran for a total of 192 min at power levels above 1 MW on two separate days. It operated at design conditions of 514 MW and an exit gas temperature of 2548 K for 40 min in two 20-min tests separated by a brief hold at low power and temperature. In all, Pewee-1 was subjected to four cycles of operation to 2448 K or above.

Pewee-1 set power density and temperature records for the nuclear rocket reactors, or any other reactor, in fact. Its power density was 20% higher than that of Phoebus 2A and ~50% above that required for the 1500-MW NERVA reactor. Its gas temperature exceeded those achieved in the NRX tests by nearly 423 K. Pewee-1 demonstrated an 825-s specific impulse.

Same type of fuel elements as Phoebus 1A.

#### March 20, 1969

The first down-firing nuclear rocket engine, XE-Prime, successfully completed an intermediate power test. Eight more tests were completed at

various power levels, one >1000 MW, for a total of 115 min of power operation. Individual test times were limited by the facility water storage system, which could not support operations much longer than 10 min at full reactor power.

This test series was a significant milestone in the nuclear rocket program, demonstrating feasibility of the NERVA concept.

#### June 1, 1972

Nuclear Furnace (NF-1), the smallest reactor tested at NRDS, operated successfully at 54-MW power through five test cycles; total operating time was 108 min.

NF-1 was designed with a remotely replaceable core in a reusable test bed, intended as an inexpensive approach to multiple testing of advance fuel materials and structures. Another special feature of this test series was evaluation of a reactor effluent cleanup system installed in the test facility. This system performed as expected in removing radioactive contaminants from the effluent reactor gas.

Two types of fuel elements were tested in NF-1. (1) Full-length, "composite," 19-hole fuel elements, (U-Zr)C-loaded to total carbide content of 35 vol%, bores coated with ZrC by CVD process. (2) Half-length, 1-hole, hexagonal carbide fuel elements, 0.64 mm (25.6 in.) long, 5.5 mm (0.220 in.) across flats, 3.2-mm (0.128-in.) bore, (U,Zr)C-loaded, with carbon: metal atom ratios of 0.8:0.92, impregnated with zirconium by CVD process and heat treated.